

UCSF

UC San Francisco Previously Published Works

Title

White matter abnormalities across different epilepsy syndromes in adults: an ENIGMA-Epilepsy study

Permalink

<https://escholarship.org/uc/item/8751p6q3>

Journal

Brain, 143(8)

ISSN

0006-8950

Authors

Hatton, Sean N
Huynh, Khoa H
Bonilha, Leonardo
et al.

Publication Date

















2020-08-01

DOI

10.1093/brain/awaa200

Peer reviewed

White matter abnormalities across different epilepsy syndromes in adults: an ENIGMA-Epilepsy study

 Sean N. Hatton,¹  Khoa H. Huynh,² Leonardo Bonilha,³ Eugenio Abela,⁴ Saud Alhusaini,^{5,6}  Andre Altmann,⁷ Marina K. M. Alvim,⁸  Akshara R. Balachandra,^{9,10}  Emanuele Bartolini,^{11,12} Benjamin Bender,¹³  Neda Bernasconi,¹⁴ Andrea Bernasconi,¹⁴ Boris Bernhardt,¹⁵ Núria Bargallo,¹⁶ Benoit Caldaïrou,¹⁴ Maria E. Caligiuri,¹⁷  Sarah J. A. Carr,¹⁸ Gianpiero L. Cavalleri,^{19,20} Fernando Cendes,⁸  Luis Concha,²¹ Esmail Davoodi-bojd,²² Patricia M. Desmond,²³ Orrin Devinsky,²⁴ Colin P. Doherty,^{25,26} Martin Domin,²⁷ John S. Duncan,^{28,29} Niels K. Focke,^{30,31} Sonya F. Foley,³²  Antonio Gambardella,^{19,33}  Ezequiel Gleichgerrcht,³ Renzo Guerrini,¹¹ Khalid Hamandi,^{34,35} Akari Ishikawa,⁸ Simon S. Keller,^{36,37} Peter V. Kochunov,³⁸ Raviteja Kotikalapudi,^{39,40} Barbara A. K. Kreilkamp,^{36,37} Patrick Kwan,^{41,42} Angelo Labate,^{17,33} Soenke Langner,^{43,44} Matteo Lenge,^{11,45} Min Liu,⁴⁶ Elaine Lui,^{23,47} Pascal Martin,³¹ Mario Mascalchi,⁴⁸ José C.V. Moreira,⁸ Marcia E. Morita-Sherman,^{8,49} Terence J. O'Brien,^{41,42,50} Heath R. Pardoe,⁵¹ José C. Pariente,¹⁶ Leticia F. Ribeiro,⁸  Mark P. Richardson,⁵²  Cristiane S. Rocha,⁸ Raúl Rodríguez-Cruces,^{15,21} Felix Rosenow,^{53,54}  Mariasavina Severino,⁵⁵ Benjamin Sinclair,^{42,50}  Hamid Soltanian-Zadeh,^{56,57}  Pasquale Striano,^{58,59}  Peter N. Taylor,⁶⁰ Rhys H. Thomas,^{61,62} Domenico Tortora,⁵⁶ Dennis Velakoulis,^{63,64} Annamaria Vezzani,⁶⁵ Lucy Vivash,^{41,42} Felix von Podewils,⁶⁶ Sjoerd B. Vos,^{67,68} Bernd Weber,⁶⁹ Gavin P. Winston,^{68,70,71} Clarissa L. Yasuda,⁸ Alyssa H. Zhu,⁷² Paul M. Thompson,⁷² Christopher D. Whelan,^{6,73} Neda Jahanshad,⁷² Sanjay M. Sisodiya,^{71,74} and Carrie R. McDonald⁷⁵

The epilepsies are commonly accompanied by widespread abnormalities in cerebral white matter. ENIGMA-Epilepsy is a large quantitative brain imaging consortium, aggregating data to investigate patterns of neuroimaging abnormalities in common epilepsy syndromes, including temporal lobe epilepsy, extratemporal epilepsy, and genetic generalized epilepsy. Our goal was to rank the most robust white matter microstructural differences across and within syndromes in a multicentre sample of adult epilepsy patients. Diffusion-weighted MRI data were analysed from 1069 healthy controls and 1249 patients: temporal lobe epilepsy with hippocampal sclerosis ($n = 599$), temporal lobe epilepsy with normal MRI ($n = 275$), genetic generalized epilepsy ($n = 182$) and non-lesional extratemporal epilepsy ($n = 193$). A harmonized protocol using tract-based spatial statistics was used to derive skeletonized maps of fractional anisotropy and mean diffusivity for each participant, and fibre tracts were segmented

using a diffusion MRI atlas. Data were harmonized to correct for scanner-specific variations in diffusion measures using a batch-effect correction tool (ComBat). Analyses of covariance, adjusting for age and sex, examined differences between each epilepsy syndrome and controls for each white matter tract (Bonferroni corrected at $P < 0.001$). Across ‘all epilepsies’ lower fractional anisotropy was observed in most fibre tracts with small to medium effect sizes, especially in the corpus callosum, cingulum and external capsule. There were also less robust increases in mean diffusivity. Syndrome-specific fractional anisotropy and mean diffusivity differences were most pronounced in patients with hippocampal sclerosis in the ipsilateral parahippocampal cingulum and external capsule, with smaller effects across most other tracts. Individuals with temporal lobe epilepsy and normal MRI showed a similar pattern of greater ipsilateral than contralateral abnormalities, but less marked than those in patients with hippocampal sclerosis. Patients with generalized and extratemporal epilepsies had pronounced reductions in fractional anisotropy in the corpus callosum, corona radiata and external capsule, and increased mean diffusivity of the anterior corona radiata. Earlier age of seizure onset and longer disease duration were associated with a greater extent of diffusion abnormalities in patients with hippocampal sclerosis. We demonstrate microstructural abnormalities across major association, commissural, and projection fibres in a large multicentre study of epilepsy. Overall, patients with epilepsy showed white matter abnormalities in the corpus callosum, cingulum and external capsule, with differing severity across epilepsy syndromes. These data further define the spectrum of white matter abnormalities in common epilepsy syndromes, yielding more detailed insights into pathological substrates that may explain cognitive and psychiatric co-morbidities and be used to guide biomarker studies of treatment outcomes and/or genetic research.

- 1 Department of Neurosciences, Center for Multimodal Imaging and Genetics, University of California San Diego, La Jolla 92093 CA, USA
- 2 Center for Multimodal Imaging and Genetics, University of California San Diego, La Jolla 92093 CA, USA
- 3 Department of Neurology, Medical University of South Carolina, Charleston 29425 SC, USA
- 4 Maurice Wohl Clinical Neuroscience Institute, Institute of Psychiatry, Psychology and Neuroscience, Kings College London, London SE5 9NU UK
- 5 Neurology Department, Yale School of Medicine, New Haven 6510 CT, USA
- 6 Molecular and Cellular Therapeutics, The Royal College of Surgeons in Ireland, Dublin, Ireland
- 7 Centre of Medical Image Computing, Department of Medical Physics and Biomedical Engineering, University College London, London WC1V 6LJ, UK
- 8 Department of Neurology, University of Campinas - UNICAMP, Campinas 13083-888 São Paulo, Brazil
- 9 Center for Multimodal Imaging and Genetics, UCSD School of Medicine, La Jolla 92037 CA, USA
- 10 Boston University School of Medicine, Boston 2118 MA, USA
- 11 Pediatric Neurology, Neurogenetics and Neurobiology Unit and Laboratories, Children’s Hospital A. Meyer-University of Florence, Florence, Italy
- 12 USL Centro Toscana, Neurology Unit, Nuovo Ospedale Santo Stefano, Prato, Italy
- 13 Department of Diagnostic and Interventional Neuroradiology, University Hospital Tübingen, Tübingen 72076, Germany
- 14 Neuroimaging of Epilepsy Laboratory, Montreal Neurological Institute, McGill University, Montreal H3A 2B4 QC, Canada
- 15 Montreal Neurological Institute, McGill University, Montreal H3A2B4 QC, Canada
- 16 Magnetic Resonance Image Core Facility, Institut d’Investigacions Biomèdiques August Pi i Sunyer (IDIBAPS), Barcelona 8036 Barcelona, Spain
- 17 Neuroscience Research Center, University Magna Graecia, viale Europa, Germaneto, 88100, Catanzaro, Italy
- 18 Neuroscience, Institute of Psychiatry, Psychology and Neuroscience, De Crespigny Park, London SE5 8AF, UK
- 19 Royal College of Surgeons in Ireland, School of Pharmacy and Biomolecular Sciences, Dublin D02 YN77 Ireland
- 20 FutureNeuro Research Centre, Science Foundation Ireland, Dublin D02 YN77, Ireland
- 21 Institute of Neurobiology, Universidad Nacional Autónoma de México, Queretaro 76230, Mexico
- 22 Radiology and Research Administration, Henry Ford Hospital, 1 Detroit 48202 MI, USA
- 23 Department of Radiology, Royal Melbourne Hospital, University of Melbourne, Melbourne 3050 Victoria, Australia
- 24 Director, NYU Epilepsy Center, New York 10016 NY, USA
- 25 Division of Neurology, Trinity College Dublin, TBSI, Pearse Street, Dublin D02 R590, Ireland
- 26 FutureNeuro SFI Centre for Neurological Disease, RCSI, St Stephen’s Green, Dublin D02 H903, Ireland
- 27 Functional Imaging Unit, University Medicine Greifswald, Greifswald 17475 M/V, Germany
- 28 Department of Clinical and Experimental Epilepsy, UCL Queen Square Institute of Neurology, Queen Square, London WC1N 3BG, UK
- 29 MRI Unit, Chalfont Centre for Epilepsy, Chalfont-St-Peter, Buckinghamshire SL9 0RJ, UK
- 30 Clinical Neurophysiology, University Medicine Göttingen, 37099 Göttingen, Germany
- 31 Department of Epileptology, University of Tübingen, 72076 Tübingen, Germany
- 32 CUBRIC, Cardiff University, Cardiff CF24 4HQ, Wales
- 33 Institute of Neurology, University Magna Graecia, 88100, Catanzaro, Italy
- 34 The Wales Epilepsy Unit, Cardiff and Vale University Health Board, Cardiff CF144XW, UK

- 35 Brain Research Imaging Centre, Cardiff University, Cardiff CF24 4HQ, UK
 36 Institute of Translational Medicine, University of Liverpool, Liverpool L69 3BX, UK
 37 Walton Centre NHS Foundation Trust, Liverpool L9 7LJ, UK
 38 Maryland Psychiatric Research Center, 55 Wade Ave, Baltimore 21228, MD, USA
 39 Department of Neurology and Epileptology, University Hospital Tübingen, Tübingen 72076 BW, Germany
 40 Department of Diagnostic and Interventional Neuroradiology, University Hospital Tübingen, Tübingen 72076 BW, Germany
 41 Department of Neuroscience, Central Clinical School, Monash University, Melbourne 3004 Victoria, Australia
 42 Department of Medicine, University of Melbourne, Royal Melbourne Hospital, Parkville 3050 Victoria, Australia
 43 Institute for Diagnostic Radiology and Neuroradiology, Ernst Moritz Arndt University Greifswald Faculty of Medicine, Greifswald 17475, Germany
 44 Institute for Diagnostic and Interventional Radiology, Pediatric and Neuroradiology, Rostock University Medical Centre, Rostock 18057, Germany
 45 Functional and Epilepsy Neurosurgery Unit, Children's Hospital A. Meyer-University of Florence, Florence 50139, Italy
 46 Department of Neurology, Montreal Neurological Institute, Montreal H3A 2B4 QC, Canada
 47 Department of Medicine and Radiology, University of Melbourne, 3Parkville 3050 Victoria, Australia
 48 Meyer Children Hospital University of Florence, Florence 50130 Tuscany, Italy
 49 Cleveland Clinic, Cleveland 44195 OH, USA
 50 Department of Neurology, Alfred Health, Melbourne 3004 Victoria, Australia
 51 Department of Neurology, New York University School of Medicine, New York City 10016 NY, USA
 52 Division of Neuroscience, King's College London, Institute of Psychiatry, London SE5 8AB, UK
 53 Epilepsy Center Frankfurt Rhine-Main, University Hospital Frankfurt, Germany, Frankfurt 60528 Hesse, Germany
 54 Center for Personalized Translational Epilepsy Research (CePTER), Goethe-University Frankfurt, Frankfurt a. M. 60528, Germany
 55 Neuroradiology Unit, IRCCS Istituto Giannina Gaslini, Genoa 16147 Liguria, Italy
 56 Radiology and Research Administration, Henry Ford Health System, Detroit 48202-2692 MI, USA
 57 School of Electrical and Computer Engineering, University of Tehran, Tehran 14399-57131, Iran
 58 IRCCS Istituto Giannina Gaslini, Genoa 16147 Liguria, Italy
 59 Department of Neurosciences, Rehabilitation, Ophthalmology, Genetics, Maternal and Child Health, University of Genova, Genova, Italy
 60 School of Computing, Newcastle University, Urban Sciences Building, Science Square, Newcastle upon Tyne NE4 5TG, UK
 61 Translational and Clinical Research Institute, Newcastle University, Newcastle upon Tyne NE2 4HH, UK
 62 Royal Victoria Infirmary, Newcastle upon Tyne NE1 4LP, UK
 63 Royal Melbourne Hospital, Melbourne 3050 Victoria, Australia
 64 University of Melbourne, Parkville, Melbourne 3050 Victoria, Australia
 65 Istituto di Ricerche Farmacologiche Mario Negri IRCCS, Milano 20156 Italy
 66 Epilepsy Center, University Medicine Greifswald, Greifswald 17489 Mecklenburg-Vorpommern, Germany
 67 Centre for Medical Image Computing, University College London, London, WC1V 6LJ, UK
 68 Epilepsy Society, MRI Unit, Chalfont St Peter, Buckinghamshire, SL9 0RJ, UK
 69 Institute of Experimental Epileptology and Cognition Research, University of Bonn, Venusberg Campus 1, Bonn 53127 NRW, Germany
 70 Department of Medicine, Division of Neurology, Queen's University, Kingston K7L 3N6 ON, Canada
 71 MRI Unit, Chalfont Centre for Epilepsy, Chalfont-St-Peter, Buckinghamshire, SL9 0RJ UK
 72 Imaging Genetics Center, Mark and Mary Stevens Institute for Neuroimaging and Informatics, USC Keck School of Medicine, Los Angeles 90232 CA, USA
 73 Research and Early Development (RED), Biogen Inc., Cambridge, MA 02139, USA
 74 Chalfont Centre for Epilepsy, Chalfont-St-Peter, SL9 0RJ Bucks, UK
 75 Department of Psychiatry, Center for Multimodal Imaging and Genetics, University of California San Diego, La Jolla 92093 CA, USA

Correspondence to: Carrie R. McDonald

Department of Psychiatry, Center for Multimodal Imaging and Genetics, University of California San Diego, 9500 Gilman Dr, La Jolla 92093 CA, USA
 E-mail: camcdonald@health.ucsd.edu

Keywords: epilepsy; diffusion tensor imaging; multisite analysis; white matter

Abbreviations: ACR = anterior corona radiata; AD = axial diffusivity; B/G/SCC = body/genu/splenium of the corpus callosum; CGC = cingulate gyrus of the cingulum bundle; CGH = parahippocampal cingulum; ExE = non-lesional extratemporal epilepsy; FA = fractional anisotropy; GGE = genetic generalized epilepsy; HS = hippocampal sclerosis; MD = mean diffusivity; RD = radial diffusivity; ROI = region of interest; SLF = superior longitudinal fasciculus; TLE-NL = non-lesional temporal lobe epilepsy

Introduction

Epilepsy affects over 50 million individuals worldwide (Bell *et al.*, 2014). Focal epilepsies account for around 60% of all adult epilepsy cases, and temporal lobe epilepsy (TLE) is the most common (Télez-Zenteno and Hernández-Ronquillo, 2012). TLE is associated with hippocampal sclerosis (HS) in 60–70% of cases (Coan and Cendes, 2013). Among adult epilepsy patients, up to 20% have genetic generalized epilepsy (GGE), with bilateral synchronous seizure onset and a presumed genetic background (Scheffer *et al.*, 2017). These epilepsy syndromes are frequently studied in isolation and may have distinct pathophysiological substrates and mechanisms. Their unique and shared biological pathways are beginning to be unravelled using population genetics (ILAE, 2018) and transcriptomics (Altmann *et al.*, 2017), paving the pathway for potential novel treatments.

Once considered primarily ‘grey matter’ diseases, brain imaging studies with diffusion MRI have helped reveal that both focal and generalized epilepsies represent network disorders with widespread white matter alterations even in the absence of visible MRI lesions (Engel *et al.*, 2013). Patients with TLE, particularly those with HS, may exhibit white matter abnormalities both proximal to and distant from the seizure focus, often most pronounced in the ipsilateral hemisphere (Focke *et al.*, 2008; Ahmadi *et al.*, 2009; Labate *et al.*, 2015; Caligiuri *et al.*, 2016). Studies in patients with GGE have demonstrated microstructural compromise in frontal and parietal regions bilaterally, and in thalamocortical pathways (Keller *et al.*, 2011; Lee *et al.*, 2014; Szaflarski *et al.*, 2016). White matter disruption in epilepsy is also linked to cognitive functioning (McDonald *et al.*, 2008; Yogarajah *et al.*, 2008, 2010) and postsurgical seizure outcomes (Bonilha *et al.*, 2015; Keller *et al.*, 2015, 2017; Gleichgerrcht *et al.*, 2018), indicating the importance of white matter networks in the pathophysiology and co-morbidities of epilepsies.

Meta-analyses and single-site studies of diffusion MRI suggest widespread microstructural abnormalities in patients with focal epilepsy affecting association, commissural, and projection fibres, whereas microstructural differences in GGE are reportedly less pronounced (Otte *et al.*, 2012; Slinger *et al.*, 2016). Unfortunately, the exact tracts, spatial pattern, and extent of damage reported varies across studies, making it hard to draw conclusions about syndrome-specific and generalized white matter abnormalities in epilepsies. Inconsistencies may be due, in part, to small sample sizes at individual centres, which may lack power to detect reliable differences across a large number of white matter tracts and multiple diffusion measures. Methods for image acquisition, processing, and tract selection also differ greatly across studies, adding other sources of variability. Few studies consider white matter abnormalities as a function of sex, age, and key clinical characteristics leading to multiple uncertainties in the findings. Although meta-analyses reduce some of these limitations, harmonizing the image processing and data analysis in a

consortia effort alleviates some of the known sources of variation and allows for the statistical modelling of other population differences. Furthermore, pooling raw data across a large number of centres in a mega-analysis may offer greater power to detect group effects and enable cross-syndrome comparisons that have not previously been possible. [A meta-analysis aggregates summary results (e.g. effect size estimates, standard errors, and confidence intervals) across studies, but a mega-analysis aggregates individual participant data across studies, and may allow additional data harmonization. For an empirical comparison between the two techniques using structural MRI data, refer to Boedhoe *et al.* (2018).] Further, due to the collation of world-wide harmonized image analysis protocols, analysis, and reporting of results, white matter differences in epilepsy can now be directly compared to those of other neurological and psychiatric disorders, highlighting pathology that may be unique to epilepsy and/or its treatments.

Enhancing NeuroImaging Genetics through Meta-Analysis (ENIGMA) is a global initiative combining individually collected samples from studies around the world into a single large-scale study, with coordinated image processing, and integrating imaging, phenotypic, and genomic data from hundreds of research centres worldwide (Thompson *et al.*, 2020). Standardized protocols for image processing, quality assurance, and statistical analyses were applied using the validated ENIGMA-diffusion MRI protocols for multisite diffusion tensor imaging (DTI) harmonization, <http://enigma.usc.edu/ongoing/dti-working-group/> (Jahanshad *et al.*, 2013; Kochunov *et al.*, 2014, 2015).

Our primary goal was to identify and rank the most robust white matter microstructural alterations across and within common epilepsy syndromes in a sample of 1249 adult epilepsy patients and 1069 healthy controls across nine countries from North and South America, Europe and Australia. First, we studied all patients in aggregate (‘all epilepsies’) compared to age- and sex-matched controls, followed by targeted analyses focusing on patients with right and left TLE-HS, right and left non-lesional TLE (TLE-NL), non-lesional extratemporal epilepsy (ExE), and GGE. We characterize effect size differences across and within these epilepsy syndromes in fractional anisotropy (FA) and mean diffusivity (MD), as well as axial (AD) and radial (RD) diffusivity. We also examine regional white matter associations with age of seizure onset and disease duration.

We hypothesized that, compared to controls, each patient group would show white matter alterations beyond the suspected epileptogenic region, with unique patterns in each group. Specifically, we hypothesized that patients with TLE would show the most pronounced alterations in ipsilateral temporo-limbic regions, most notably in TLE-HS. We hypothesized that patients with GGE would show bilateral fronto-thalamocortical alterations. We also hypothesized that common white matter alterations would emerge across the patient groups and that many of these regional alterations would correlate with years of disease duration.

Table 1 Characteristics of the patient and control samples by site

Centre	Age controls		Age cases		Age of onset		Duration of illness		Total controls	Total cases	L TLE-HS cases	R TLE-HS cases	L TLE-NL cases	R TLE-NL cases	GGE cases	ExE cases	Total n
	Mean ± SD	Mean ± SD	Mean ± SD	Mean ± SD	Mean ± SD	Mean ± SD											
Bonn	38.0 ± 14.0	41.8 ± 12.9	17.7 ± 11.6	23.8 ± 14.2	44	64	42	22	0	0	0	0	0	0	0	0	108
CUBRIC	28.3 ± 8.4	28.6 ± 7.7	14.7 ± 4.0	14.0 ± 9.5	35	34	0	0	0	0	0	0	0	0	34	0	69
EKUT	40.0 ± 14.9	33.9 ± 13.1	19.3 ± 14.2	14.6 ± 10.4	19	15	0	0	0	0	0	0	0	0	15	0	34
EPICZ	38.6 ± 11.2	38.3 ± 9.7	19.1 ± 12.4	19.2 ± 12.5	113	86	19	26	26	15	0	0	0	0	0	0	199
EPiGEN_Ireland	34.8 ± 9.5	35.9 ± 9.0	19.1 ± 10.9	18.1 ± 12.9	67	47	9	5	17	16	0	0	0	0	0	0	114
Florence	34.6 ± 11.6	37.6 ± 13.5	14.0 ± 7.4	19.0 ± 9.9	35	4	0	0	0	0	0	0	0	0	0	2	39
Genova	25.3 ± 8.2	25.3 ± 8.2	10.4 ± 4.6	14.7 ± 7.7	20	17	0	1	3	4	7	2	3	4	7	2	37
Greifswald	n/a	34.6 ± 14.0	19.2 ± 9.7	15.4 ± 9.2	n/a	48	0	0	0	0	0	0	0	0	35	13	48
HFHS_2.6mm	29.5 ± 7.0	38.3 ± 13.0	19.0 ± 16.9	19.0 ± 12.9	21	57	6	8	8	7	0	28	7	0	0	28	78
HFHS_3mm	n/a	40.1 ± 15.4	–	–	0	14	3	3	3	3	0	2	3	0	0	2	14
IDIBAPS_3IDir	n/a	39.3 ± 10.1	22.5 ± 13.4	16.4 ± 11.1	0	25	5	7	3	2	1	7	2	1	1	7	25
IDIBAPS_39Dir	32.4 ± 6.6	33.3 ± 9.4	16.9 ± 11.8	17.6 ± 11.9	30	19	3	8	0	1	1	6	0	1	1	6	49
IDIBAPS_88Dir	34.1 ± 5.1	37.6 ± 10.5	15.6 ± 11.0	22.0 ± 13.3	22	27	5	10	3	3	0	6	3	0	0	6	49
KCL	30.4 ± 7.5	35.0 ± 9.5	–	–	92	89	24	38	0	0	27	0	0	0	27	0	181
Liverpool_Walton	31.8 ± 7.7	31.1 ± 10.3	14.3 ± 8.8	16.7 ± 11.9	40	33	5	3	8	5	1	11	5	1	1	11	73
Melbourne	n/a	37.2 ± 9.9	22.4 ± 12.8	14.8 ± 11.2	0	25	13	5	6	1	0	0	6	1	0	0	25
MNI	30.7 ± 7.4	32.1 ± 9.5	16.4 ± 9.6	15.4 ± 10.6	46	149	20	22	23	15	0	69	15	0	0	69	195
MUSC	55.2 ± 6.6	36.6 ± 10.7	18.5 ± 13.5	17.8 ± 12.1	58	43	19	6	11	7	0	0	11	7	0	0	101
NYU	30.3 ± 10.0	32.6 ± 8.9	24.0 ± 12.7	8.6 ± 9.9	26	45	2	2	8	3	0	30	3	0	0	30	71
UCL	37.7 ± 12.4	38.7 ± 11.4	13.9 ± 10.7	24.7 ± 14.3	29	53	24	13	6	10	0	0	6	10	0	0	82
UCSD	37.3 ± 13.5	34.0 ± 11.9	19.6 ± 12.9	15.2 ± 13.3	47	55	17	12	13	13	0	0	13	0	0	0	102
UMG	36.0 ± 10.4	34.1 ± 10.8	16.6 ± 8.1	15.6 ± 11.7	20	36	2	5	0	0	24	5	0	0	24	5	56
UNAM	33.7 ± 12.2	31.4 ± 11.7	15.8 ± 11.1	15.5 ± 12.8	34	30	9	10	9	2	0	0	9	2	0	0	64
UNICAMP	35.5 ± 10.8	40.6 ± 9.9	12.3 ± 9.6	28.3 ± 12.2	271	234	92	74	15	4	37	12	15	4	37	12	505
Combined	35.5 ± 11.7	36.1 ± 11.2	16.3 ± 11.3	19.9 ± 13.0	1069	1249	319	280	162	113	182	193	162	113	182	193	2318

n/a = not available.

Table 2 Demographic and clinical characteristics of the total sample

	<i>n</i>	Age (SD)	Sex, % male	Age of onset (SD)	Duration of illness (SD)
Controls	1069	35.5 (11.7)	41.7	–	–
All patients	1249	36.1 (11.2)	42.9	16.3 (11.3)	19.9 (13.0)
Left TLE-HS	319	38.3 (10.6)	43.3	14.5 (11.5)	24.2 (13.3)
Right TLE-HS	280	39.3 (10.8)	42.5	15.3 (11.6)	24.1 (13.9)
Left TLE-NL	162	36.1 (10.9)	38.3	18.8 (11.6)	17.1 (12.1)
Right TLE-NL	113	35.1 (11.4)	37.2	19.5 (12.2)	15.1 (11.2)
GGE	182	31.8 (9.9)	44.5	14.8 (7.3)	16.8 (10.5)
ExE	193	32.7 (11.5)	43.5	17.6 (11.1)	15.1 (11.5)

Post hoc comparisons revealed that controls were younger than both TLE-HS groups and older than patients with GGE and ExE (all *P*-values < 0.05). Both TLE-HS groups and the left TLE-NL group were older than the GGE and ExE groups (*P* < 0.05). The right TLE-HS group was older than both TLE-NL groups (*P* < 0.05).

Materials and methods

All study participants provided written informed consent for the local study, and the local institutional review boards and ethics committees approved each included cohort study.

Study sample

This study from the ENIGMA-Epilepsy working group consists of 21 cohorts from nine different countries and includes diffusion MRI scans from 1069 healthy controls and 1249 adult epilepsy patients. Demographic and clinical characteristics of the samples are presented in Table 1 (by site) and Table 2 (across site). An epilepsy specialist assessed seizure and syndrome classifications at each centre, using the International League Against Epilepsy (ILAE) criteria. For the TLE subgroups, we included anyone with the typical electroclinical constellation of this syndrome (Berg *et al.*, 2010). All TLE-HS patients had a neuroradiologically-confirmed diagnosis of unilateral hippocampal atrophy and increased T₂ signal on clinical MRI, whereas all TLE-NL patients had a normal MRI undertaken at the same time as the analysed diffusion MRI scan. Participants with a normal MRI and frontal, occipital, or parietal epilepsy were labelled as ExE. Participants with tonic-clonic, absence or myoclonic seizures with generalized spike-wave discharges on EEG were included in the GGE group. Data on anti-epilepsy drug (AED) regimen, seizure frequency, and clinical outcomes (e.g. drug resistance, postsurgical outcome) were not available at the time of the analysis. We excluded participants who did not meet criteria for one of the above epilepsy syndromes or who had MRI-visible lesions that would disrupt brain morphometry, including malformations of cortical development, tumours or prior neurosurgery. Participants were between 18 and 70 years of age.

Image processing and analysis

Scanner descriptions and acquisition protocols for all sites are provided in Supplementary Table 1. Individual scanners that used different acquisition protocols are listed as separate scanner instances. Each site conducted the preprocessing of diffusion-weighted images, including eddy current correction, echo-planar imaging (EPI)-induced distortion correction, and tensor estimation. Next, diffusion-tensor imaging (DTI) images were processed using the ENIGMA-DTI protocols. These image processing and quality control protocols are freely available at the ENIGMA-DTI (<http://enigma.ini.usc.edu/ongoing/dti-working-group/>) and NITRC (https://www.nitrc.org/projects/enigma_dti/) webpages. Measures of FA, MD, AD and RD were obtained for 38 regions of interest (ROIs) using the Johns Hopkins University (JHU) atlas (Fig. 1).

For analyses of all patients and for each syndrome, we used the left and right tracts, the midline structures of the body (BCC), genu (GCC), and splenium (SCC) of the corpus callosum and the average diffusion metric (FA/MD/AD/RD) across the whole brain (38 ROIs). Corrections for multiple comparisons were carried out for each epilepsy syndrome, based on the number of ROIs: 34 bilateral white matter regions + BCC + GCC + SCC + Average FA = 38 ROIs; Bonferroni-corrected threshold for significance $P = 0.05/38 = 0.001$.

For analyses of all patients and for each syndrome, we used the left and right tracts, the midline structures of the body (BCC), genu (GCC), and splenium (SCC) of the corpus callosum and the average diffusion metric (FA/MD/AD/RD) across the whole brain (38 ROIs). Corrections for multiple comparisons were carried out for each epilepsy syndrome, based on the number of ROIs: 34 bilateral white matter regions + BCC + GCC + SCC + Average FA = 38 ROIs; Bonferroni-corrected threshold for significance $P = 0.05/38 = 0.001$.

Data harmonization

The batch-effect correction tool, ComBat, was used to harmonize between-site and between-protocol variations in diffusion metrics as previously demonstrated (Fortin *et al.*, 2017). The method globally rescales the data (all ROIs for FA, MD, RD or AD separately) for each scanner instance using a *z*-score transformation map common to all features. ComBat uses an empirical Bayes framework (Johnson *et al.*, 2007) to improve the variance of the parameter estimates, assuming that all ROIs share the same common distribution. Thus, all ROIs are used to inform the statistical properties of the scanner effects. We set each scanner instance as each individual scanner used in the collection of magnetic resonance exams, and where there were different scanning protocols used on the same scanner, each protocol was set as a different scanning instance. Scanner type was used as the batch effect and diagnosis (patients versus controls) and syndrome (GGE, TLE-HS, TLE-NL, and ExE) were used as the biological phenotypes of interest. This technique has been recently applied in other ENIGMA DTI investigations of brain disorders (Villalón-Reina *et al.*, 2019; Zavaliangos-Petropulu *et al.*, 2019).

Statistical analysis

Statistical analysis was performed in the Statistical Package for the Social Sciences (SPSS v26.0). Pearson correlation examined the association between age of onset and disease duration. ANOVA was used to test for differences in demographic and clinical characteristics among the epilepsy syndromes. To test for differences between syndromes and controls and to test for global effects of age at scan and sex on white matter, multivariate

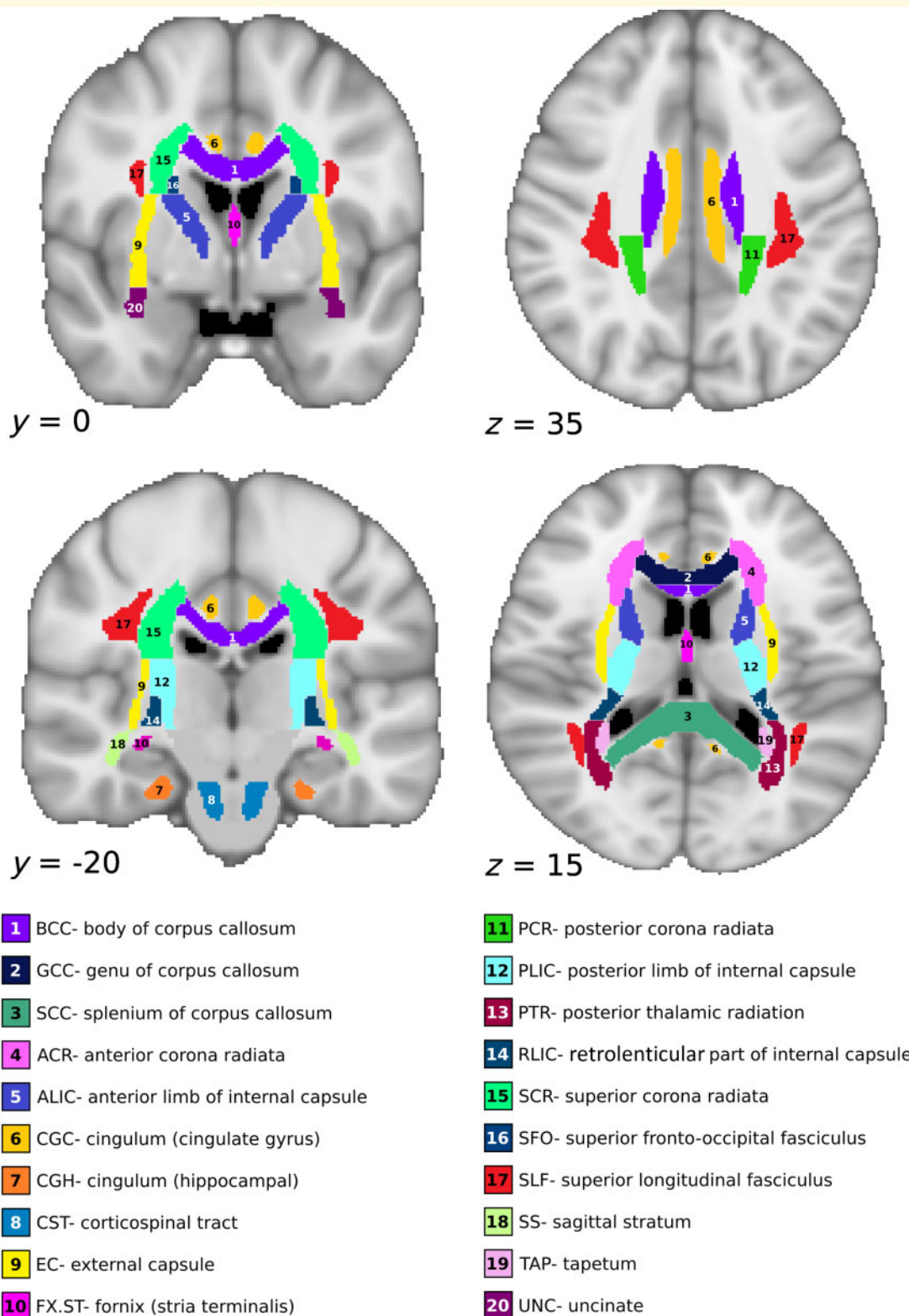


Figure 1 Fibre atlas.

analysis of covariance (MANCOVA) was performed per diffusion metric, adjusting for age, age² and sex. Age² was included in all analyses to model the non-linear effects of age on

diffusivity measures (Lebel *et al.*, 2012). ANCOVAs were then performed of each patient syndrome compared to controls controlling for age, age² and sex and Bonferroni corrected at

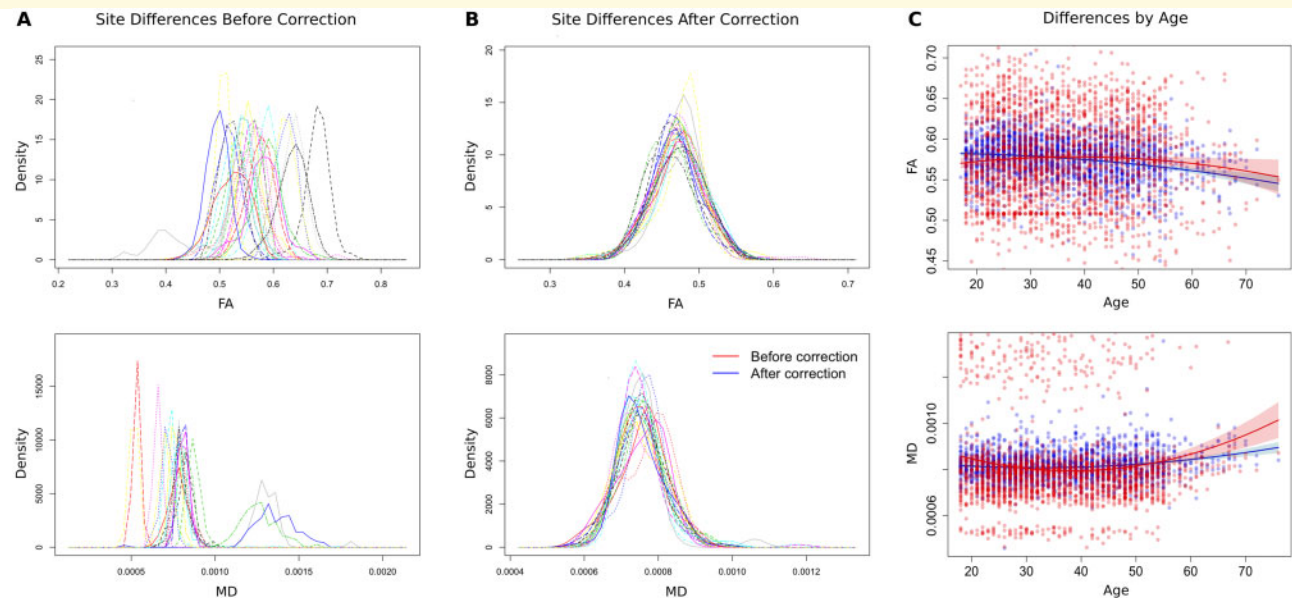


Figure 2 Diffusion MRI harmonization using ComBat. Average FA (top) and MD (bottom) measures across 24 scanners showing differences in mean FA measures per scanner (left) which are harmonized using ComBat (middle). The process corrects the variance in scanner without altering the biological variance expected with age (right). Red = before correction; Blue = after correction.

$P < 0.001$. Cohen's d effect sizes were calculated for each right and left fibre tract between controls and each patient syndrome based on the estimated marginal means (adjusted for age, age², and sex) and interpreted according to the following criteria: small $d = 0.20$ – 0.49 ; medium $d = 0.50$ – 0.79 ; large $d \geq 0.80$ (Sawilowsky, 2008). Throughout the text and figures, positive effect size values correspond to patients having higher values than controls, whereas negative effect size values correspond to patients having lower values relative to controls. Partial correlations controlling for the same covariates were performed to evaluate the relationship between each fibre tract FA/MD and age of seizure onset and disease duration (corrected $P < 0.001$). To demonstrate the most robust group differences, only tracts that showed medium and large effects are described in the text. Tracts with small effects are detailed in the [Supplementary material](#) (see [Supplementary Tables 4–7](#) and [Supplementary Figs 1 and 2](#) for all results). In a follow-up analysis to check that heteroscedasticity was not influencing results, FSL PALM (Winkler *et al.*, 2014) was used to test if permutation testing of the difference in FA between patients and controls was similar to the core ANCOVA results ([Fig. 3](#) and [Supplementary Table 4](#)). The model controlled for age and sex and 10 000 permutations were run with exchangeability blocks (Winkler *et al.*, 2015) set for permutations to take place within scanner instances only. We used the Aspin-Welch v test statistic and the simulated significance $P(\text{sim})$ threshold was set at $P < 0.001$.

Data availability

The data that support the findings of this study are available on request from the corresponding author. The data are not all publicly available in a repository as they contain information that could compromise the privacy of research participants.

Although there are data sharing restrictions imposed by (i) ethical review boards of the participating sites, and consent documents; (ii) national and trans-national data sharing law, such as GDPR; and (iii) institutional processes, some of which require a signed MTA for limited and predefined data use, we welcome sharing data with researchers, requiring only that they submit an analysis plan for a secondary project to the leading team of the Working Group (<http://enigma.ini.usc.edu>). Once this analysis plan is approved, access to the relevant data will be provided contingent on data availability and local PI approval and compliance with all supervening regulations. If applicable, distribution of analysis protocols to sites will be facilitated.

Results

Demographics

Demographic and clinical characteristics of each sample are presented in [Table 2](#). A one-way ANOVA with group as the between-subjects factor revealed differences across the seven groups in age [$F(6,2083) = 13.3$, $P < 0.001$]. Two, one-way ANOVAs across the six patient syndromes revealed group differences in age of seizure onset [$F(5,1095) = 6.3$, $P < 0.001$] and disease duration [$F(5,1039) = 22.4$, $P < 0.001$]. *Post hoc* comparisons revealed that controls were younger than both TLE-HS groups and older than patients with GGE and ExE (all P -values < 0.05). Both TLE-HS groups and the left TLE-NL group were older than the GGE and ExE groups ($P < 0.05$). The right TLE-HS group was older than both TLE-NL groups ($P < 0.05$). The GGE and TLE-HS groups had an earlier age of seizure onset

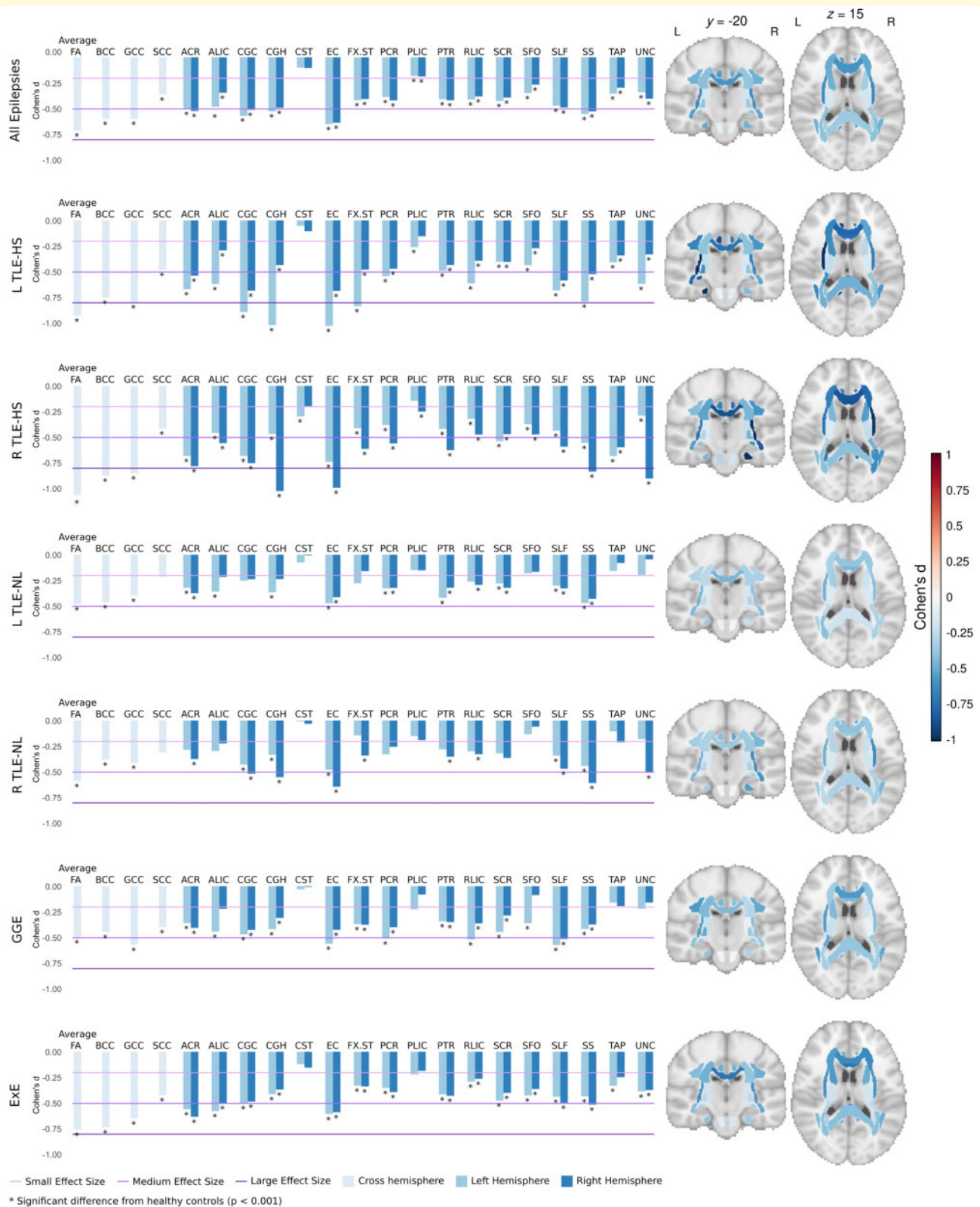


Figure 3 FA effect size bar graphs. ALIC = anterior limb of the internal capsule; CST = corticospinal tract; EC = external capsule; FX.ST = fornix/stria terminalis; L = left; PCR = posterior corona radiata; PLIC = posterior limb of the internal capsule; PTR = posterior thalamic radiation; R = right; RLIC = retrolenticular part of the internal capsule; SCR = superior corona radiata; SFO = superior fronto-occipital fasciculus; SS = sagittal stratum; TAP = tapetum; UNC = uncinata.

than the TLE-NL groups. Duration of illness in TLE-HS groups was longer than in all other groups.

Data harmonization with ComBat

Initial frequency plots revealed high variability in the distribution of diffusivity measures (e.g. mean FA, mean MD) among scanner instances (Fig. 2A). After batch correction with ComBat, the distributions were centred around a common mean (Fig. 2B), but maintained their expected association with age (Fig. 2C). Following this process, extreme ROI outliers beyond 3 standard deviations (SD) were removed from the subsequent analysis (i.e. per ROI for a given subject, not per subject). This approach resulted in the removal of only one to five ROIs per site, per diffusion parameter. The harmonization process successfully reduced the variance of diffusivity measures, especially in MD, AD and RD (Supplementary Table 2).

All epilepsies group

Multivariate tests of within-subject effects

Comparing the whole epilepsy group with healthy controls, significant differences were observed in FA [$F(228,13452) = 4.7$, $P < 0.001$, Pillai's trace = 0.44, partial $\eta^2 = 0.07$], MD [$F(228,11688) = 2.8$, $P < 0.001$, Pillai's trace = 0.31, partial $\eta^2 = 0.05$], RD [$F(228,11790) = 3.28$, $P < 0.001$, Pillai's trace = 0.36, partial $\eta^2 = 0.06$], and AD [$F(228,11946) = 1.96$, $P < 0.001$, Pillai's trace = 0.22, partial $\eta^2 = 0.04$]. Sex, age, and age² all significantly contributed to the model (Supplementary Table 3). Compared to females, males generally had higher FA, slightly higher RD and no difference in MD or AD.

All epilepsies versus healthy controls

The 'all epilepsies' group showed lower FA than controls globally in 36 of 38 ROIs ($P < 0.001$; Fig. 3 and Supplementary Table 4), with medium effect size observed for the average FA ($d = -0.71$), external capsule (left $d = -0.64$, right $d = -0.63$), body ($d = -0.59$) and genu ($d = -0.59$) of the corpus callosum (BCC and GCC), cingulate gyrus of the cingulum bundle (CGC, left $d = -0.57$, right $d = -0.50$), sagittal stratum (left $d = 0.55$, right $d = 0.52$), anterior corona radiata (ACR, left $d = -0.50$, right $d = -0.52$), and left parahippocampal cingulum (CGH, $d = -0.52$). Follow-up permutation testing confirmed that the same ROIs were significantly lower in FA in patients compared to controls when accounting for possible heteroscedasticity between scanner instances (Supplementary Table 16).

The 'all epilepsies' group showed higher MD than the controls in 27 ROIs (Fig. 4 and Supplementary Table 5). Similar to the MD, patients showed higher RD in 34 ROIs (Supplementary Fig. 1 and Supplementary Table 6) with a medium-sized effect seen in the right external capsule ($d = 0.52$). Higher AD was observed in eight ROIs (Supplementary Fig. 2 and Supplementary Table 7).

Age of onset and disease duration

Earlier age of seizure onset was significantly correlated (all P -values < 0.001) with longer disease duration across all patients ($r = -0.58$) and within each syndrome: GGE ($r = -0.39$), left TLE-HS ($r = -0.65$), right TLE-HS ($r = -0.66$), left TLE-NL ($r = -0.57$), right TLE-NL ($r = -0.54$), and ExE ($r = -0.54$).

Across all epilepsy patients, earlier age of onset was associated with lower FA across 28 ROIs ($r = 0.1$ to 0.3 , $P < 0.001$), higher MD in 16 ROIs, and higher RD in 28 ROIs (Supplementary Tables 8, 10 and 12). The most robust associations were observed between an earlier age of seizure onset and lower FA in the average FA, GCC, and bilateral external capsule, and CGC (r 's between 0.16 and 0.19). There were no significant relationships between age of onset and AD in the 'all epilepsies' group (Supplementary Table 14).

Across all epilepsy patients, disease duration showed significant associations with diffusivity measures (Supplementary Tables 9, 11, 13 and 15). A longer disease duration was associated with lower FA in 14 ROIs, increased MD in nine ROIs, and increased RD in 27 ROIs. Of note, longer disease duration was associated with lower FA in BCC, CGC, and external capsule, and with lower Average FA (r 's = -0.15 to -0.17). There were no significant relationships between disease duration and AD in all patients.

TLE-HS group

TLE-HS patients versus healthy controls

Left TLE-HS patients ($n = 319$) showed significantly lower FA than controls in 35 of 38 ROIs (Fig. 3, Supplementary Table 4), with large effect size differences in the left external capsule ($d = -1.02$), left CGH ($d = -1.01$), Average FA ($d = -0.92$), left CGC ($d = -0.89$), and left fornix/stria terminalis (FX/ST, $d = -0.83$).

Medium-sized effects were observed in GCC ($d = -0.79$), left sagittal stratum ($d = -0.78$), BCC ($d = -0.75$), right CGC ($d = -0.68$), right external capsule ($d = -0.68$), left superior longitudinal fasciculus (SLF, $d = -0.67$), left ACR ($d = -0.66$), left anterior limb of the internal capsule (ALIC, $d = -0.61$), left retrolenticular portion of the internal capsule (RLIC, $d = -0.61$), left uncinate ($d = -0.61$), right SLF ($d = -0.58$), left posterior corona radiata (PCR; $d = -0.54$), right ACR ($d = -0.53$), and right sagittal stratum ($d = -0.52$).

Significantly higher MD was observed in 28 ROIs (Fig. 4 and Supplementary Table 5), with medium-sized effects in the left external capsule ($d = 0.69$), left sagittal stratum ($d = 0.66$), and average MD ($d = 0.55$). Left TLE-HS patients showed significantly higher RD in 33 of 38 ROIs (Supplementary Fig. 1 and Supplementary Table 6). A large effect of higher RD was observed for the left external capsule ($d = 0.83$), and medium-sized effects were seen for the left sagittal stratum ($d = 0.79$), left CGC ($d = 0.69$), left CGH ($d = 0.67$), average RD ($d = 0.66$), right external capsule ($d = 0.61$), left FX/ST ($d = 0.59$), left ACR ($d = 0.57$),

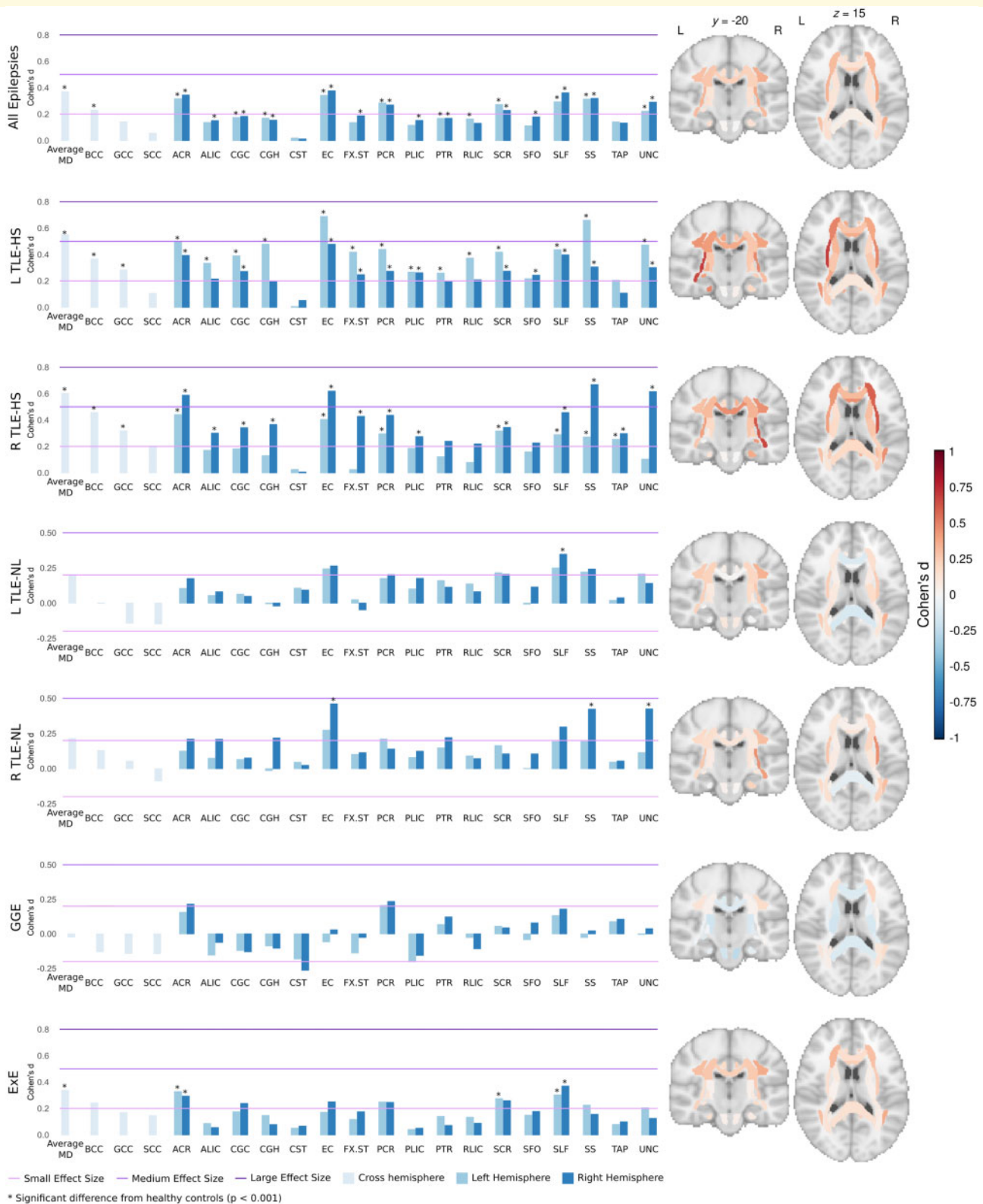


Figure 4 MD effect size bar graphs. ALIC = anterior limb of the internal capsule; CST = corticospinal tract; EC = external capsule; FX.ST = fornix/stria terminalis; L = left; PCR = posterior corona radiata; PLIC = posterior limb of the internal capsule; PTR = posterior thalamic radiation; R = right; RLIC = rentrolenticular part of the internal capsule; SCR = superior corona radiata; SFO = superior fronto-occipital fasciculus; SS = sagittal stratum; TAP = tapetum; UNC = uncinate.

SLF (left $d = 0.56$, right $d = 0.53$), right ACR ($d = 0.52$), and left RLIC ($d = 0.51$). Higher AD was observed in five ROIs (Supplementary Fig. 2 and Supplementary Table 7).

Right TLE-HS patients ($n = 280$) showed lower FA than controls in 26 of 38 ROIs ($P < 0.001$; Fig. 3 and Supplementary Table 4), with large effects observed for the average FA ($d = -1.06$), right CGH ($d = -1.02$), right external capsule ($d = -0.99$), right uncinate ($d = -0.90$), BCC ($d = -0.87$), GCC ($d = -0.85$) and right sagittal stratum ($d = -0.83$). Medium-sized effects were observed in the right ACR ($d = -0.78$), right CGC ($d = -0.73$), left external capsule ($d = -0.68$), left ACR ($d = -0.68$), left CGC ($d = -0.68$), left tapetum ($d = -0.68$), right posterior thalamic radiation ($d = -0.62$), right FX/ST ($d = -0.61$), right SLF ($d = -0.59$), right tapetum ($d = -0.59$), right ALIC ($d = -0.55$), right PCR ($d = -0.55$), left sagittal stratum ($d = -0.55$), and left superior corona radiata ($d = -0.53$).

Higher MD in the patient group were observed in 23 ROIs (Fig. 4 and Supplementary Table 5), with medium-sized effects shown in the right sagittal stratum ($d = 0.67$), right external capsule ($d = 0.62$), right uncinate ($d = 0.62$), average MD ($d = 0.60$) and right ACR ($d = 0.59$). Significantly higher RD in the patient group were observed in 31 ROIs (Supplementary Fig. 1 and Supplementary Table 6), with a large effect observed for the right external capsule ($d = 0.84$), and medium effects seen for the right sagittal stratum ($d = 0.76$), right uncinate ($d = 0.72$), average RD ($d = 0.70$), right ACR ($d = 0.69$), left external capsule ($d = 0.63$), right SLF ($d = 0.62$), right CGH ($d = 0.61$), right CGC ($d = 0.57$), BCC ($d = 0.56$), right FX/ST ($d = 0.52$), and left ACR ($d = 0.51$). Higher AD was observed in six ROIs (Supplementary Fig. 2 and Supplementary Table 7).

Age of onset and disease duration

For left TLE-HS, earlier age of onset was associated with lower FA in four ROIs, including the average FA, BCC, GCC, and left external capsule. Earlier age of seizure onset was associated with higher RD in two ROIs (Supplementary Tables 8 and 12). There was no detected relationship between age of onset and either MD or AD in the left TLE-HS group (Supplementary Tables 10 and 14).

For right TLE-HS, earlier age of onset was related to lower FA across nine ROIs, including the average FA, BCC, SCC, right external capsule, left and right CGH, right PCR, and right SLF, increased MD in seven ROIs, and increased RD in seven ROIs (Supplementary Tables 8, 10 and 12). There was no detected relationship between age of onset and AD in the TLE-HS groups (Supplementary Table 14).

For left TLE-HS patients, longer disease duration was associated with lower FA in four ROIs (BCC, bilateral CGC, and left external capsule) and higher RD in one ROI (left sagittal stratum). There were no significant relationships between disease duration and MD or AD (Supplementary Tables 9, 11, 13 and 15). For right TLE-HS, longer disease duration was associated with lower FA in eight ROIs (average FA and SCC, bilateral tapetum, and right CGH, external

capsule, PCR, and uncinate), higher MD in six ROIs, and higher RD in 10 ROIs.

TLE-NL group

TLE-NL versus healthy controls

The left TLE-NL patients ($n = 162$) showed lower FA than controls in 20 ROIs (Fig. 3 and Supplementary Table 4), higher MD in one ROI (Fig. 4 and Supplementary Table 5), and higher RD in six ROIs (Supplementary Fig. 1 and Supplementary Table 6). No significant effects of AD were detected (Supplementary Fig. 2 and Supplementary Table 7).

Right TLE-NL patients ($n = 113$) showed significantly lower FA than controls in 19 ROIs ($P < 0.001$; Fig. 3 and Supplementary Table 4), with medium-sized effects observed in the right external capsule ($d = -0.64$), right sagittal stratum ($d = -0.60$), average FA ($d = -0.58$), right CGH ($d = -0.55$), right CGC ($d = -0.51$) and right uncinate ($d = -0.50$). MD was increased in three ROIs ($P < 0.001$, Fig. 4 and Supplementary Table 5), specifically the right external capsule ($d = 0.46$), right uncinate ($d = 0.42$) and right sagittal stratum ($d = 0.42$). Significantly higher RD was observed in four ROIs (Supplementary Fig. 1 and Supplementary Table 6), with a medium-sized effect shown in the right external capsule ($d = 0.50$). No significant effects of AD were detected (Supplementary Fig. 2 and Supplementary Table 7).

Age of onset and disease duration

For left TLE-NL, no diffusivity measure was associated with earlier age of onset or duration of illness (Supplementary Tables 8–15).

For right TLE-NL patients, younger age of onset and was related to lower FA in the right uncinate ($r = 0.30$, $P < 0.001$), but not MD, AD, or RD (Supplementary Tables 8, 10, 12 and 14). Disease duration was also associated with decreased FA in the right uncinate ($r = -0.37$, $P < 0.001$), but not MD, AD, or RD (Supplementary Tables 9, 11, 13 and 15).

GGE group

GGE patients versus healthy controls

GGE patients ($n = 113$) showed significantly lower FA than controls in 28 ROIs ($P < 0.001$; Fig. 3 and Supplementary Table 4), with medium-sized effects observed in the GCC ($d = -0.57$), left SLF ($d = -0.57$), left external capsule ($d = -0.55$), left RLIC ($d = -0.51$), right SLF ($d = -0.51$) and left PCR ($d = -0.50$). GGE patients showed higher RD in four ROIs ($P < 0.001$, Supplementary Fig. 1 and Supplementary Table 6). No significant effects were seen for MD or AD (Fig. 4, Supplementary Fig. 2 and Supplementary Tables 5 and 7).

Age of onset and disease duration

For GGE patients, there was no significant association between diffusivity measures and either age of onset of epilepsy or its duration.

ExE group

ExE patients versus healthy controls

ExE patients ($n = 193$) showed significantly lower FA than controls in 33 ROIs ($P < 0.001$; Fig. 1 and Supplementary Table 4), with medium-sized effects observed for average FA ($d = -0.75$), BCC ($d = -0.65$), GCC ($d = -0.64$), right ACR ($d = -0.63$), bilateral external capsule (left $d = -0.60$, right $d = -0.58$), left ALIC ($d = -0.57$), left ACR ($d = -0.55$), and right sagittal stratum ($d = -0.51$). Higher MD was observed in six ROIs ($P < 0.001$, Fig. 4 and Supplementary Table 5) and RD in 22 ROIs ($P < 0.001$, Supplementary Fig. 1 and Supplementary Table 6). No significant effects were seen in AD (Supplementary Fig. 2 and Supplementary Table 7).

Age of onset and disease duration

For ExE patients, there were no significant associations between diffusivity measures and either age of onset of epilepsy, or its duration.

Cross-syndrome comparisons

Post hoc comparisons were conducted across the syndromes in the five ROIs that showed the largest effect size in the ‘all epilepsies’ analysis, namely average FA/MD, ACR, BCC, CGC, and external capsule averaged across hemispheres (Fig. 5). ANCOVAs, adjusting for age, age², sex, age of seizure onset, and disease duration revealed significant group differences in average FA [$F(5,874) = 3.8$, $P < 0.05$], as well as FA of the CGC [$F(5,874) = 5.0$, $P < 0.05$] and external capsule [$F(5,874) = 5.8$, $P < 0.05$].

There were differences across syndromes for the average MD [$F(5,874) = 5.3$, $P < 0.05$], ACR [$F(5,874) = 3.8$, $P < 0.05$], BCC [$F(5,874) = 4.9$, $P < 0.05$], CGC [$F(5,874) = 4.2$, $P < 0.05$], and the external capsule [$F(5,874) = 6.2$, $P < 0.05$]. Patients with left and right TLE-HS generally showed lower FA and higher MD than TLE-NL patients, as well as lower FA/higher MD than GGEs in CGC and the external capsule. The non-lesional groups (GGE, TLE-NL, and ExE) did not differ from one another.

Comparisons with other disorders

Given the many common white matter FA differences observed across epilepsy syndromes, the question arises as to whether these effects are specific to epilepsy or also seen with other brain disorders. Figure 6 displays effect size differences observed in the ‘all epilepsies’ group ($n = 1249$) relative to findings from four other ENIGMA working groups: schizophrenia ($n = 1984$; mean age, 36.2; 67% male), 22q11 syndrome ($n = 334$; mean age, 16.9; 54% male), bipolar disorder ($n = 1482$; mean age, 39.6; 39.3% male), and major depressive disorder ($n = 921$; mean age, 40.7; 39% male). The magnitude of the effect sizes were typically larger in epilepsy, compared to the other disorders for most white matter regions. Across the white matter regions, effect sizes in patients with epilepsy were significantly correlated with

those in patients with bipolar disorder (Spearman’s rho $r = 0.53$, $P < 0.05$), schizophrenia ($r = 0.53$, $P < 0.05$), and major depressive disorder ($r = 0.44$, $P < 0.05$).

Approach for multiple comparisons correction

Regional differences in diffusion parameters between syndromes and healthy controls were expressed as effect size (Cohen’s d). To identify significant differences we adopted a Bonferroni correction that adjusted for testing 38 ROIs for each syndrome ($P < 0.001$). However, an even more conservative approach corrects for each of the four diffusion metrics across the seven epilepsy syndromes. Implementing this very conservative Bonferroni cut-off would result in a threshold of $P < 0.05/(38 \times 7 \times 4) = 4.7 \times 10^{-5}$. The combination of the large sample size and the observed medium to large effect sizes in the study results in most regional differences remaining significant even at the very conservative P -value threshold. However, in contrasts involving a smaller number of patients (controls compared to GGE or TLE-NL, for example) more regions would lose the ‘significant’ label due to the reduced statistical power. Despite these few exceptions, the exact P -value cut-off does not alter the main finding that there were widespread white matter abnormalities across epilepsy syndromes. We report all effect sizes and P -values in the Supplementary material for researchers interested in examining these results with alternate definitions of statistical significance.

Discussion

This multisite DTI study in epilepsy compared data from 1249 patients with common epilepsy syndromes to 1069 healthy controls. Data were acquired at 21 sites across North America, South America, Europe, and Australia and harmonized using the same post-processing pipeline and batch effect harmonization tool.

Our results reveal marked white matter alterations across epilepsy syndromes compared to controls, with varying magnitude of FA reduction and increased MD and RD. Effects were pronounced in patients with TLE-HS and modest in GGE. In TLE-HS, the greatest changes were seen ipsilateral to the seizure focus, implying a local effect. Notably, the magnitude of the diffusion changes was greater in epilepsy than that seen in schizophrenia, bipolar disorder and major depressive disorder. The biological basis of reduced FA is considered primarily loss of axons and myelin sheaths, with increased RD and MD reflecting myelin disruption and increased extracellular space (Arfanakis et al., 2002; Concha et al., 2009). This raises the critical question of whether these diffusion abnormalities reflect the underlying pathologies that predispose to epilepsy, or if they are the consequence of epilepsy and are a biomarker of secondary damage. Since changes were more pronounced in those with a younger age of onset and longer duration of epilepsy, we

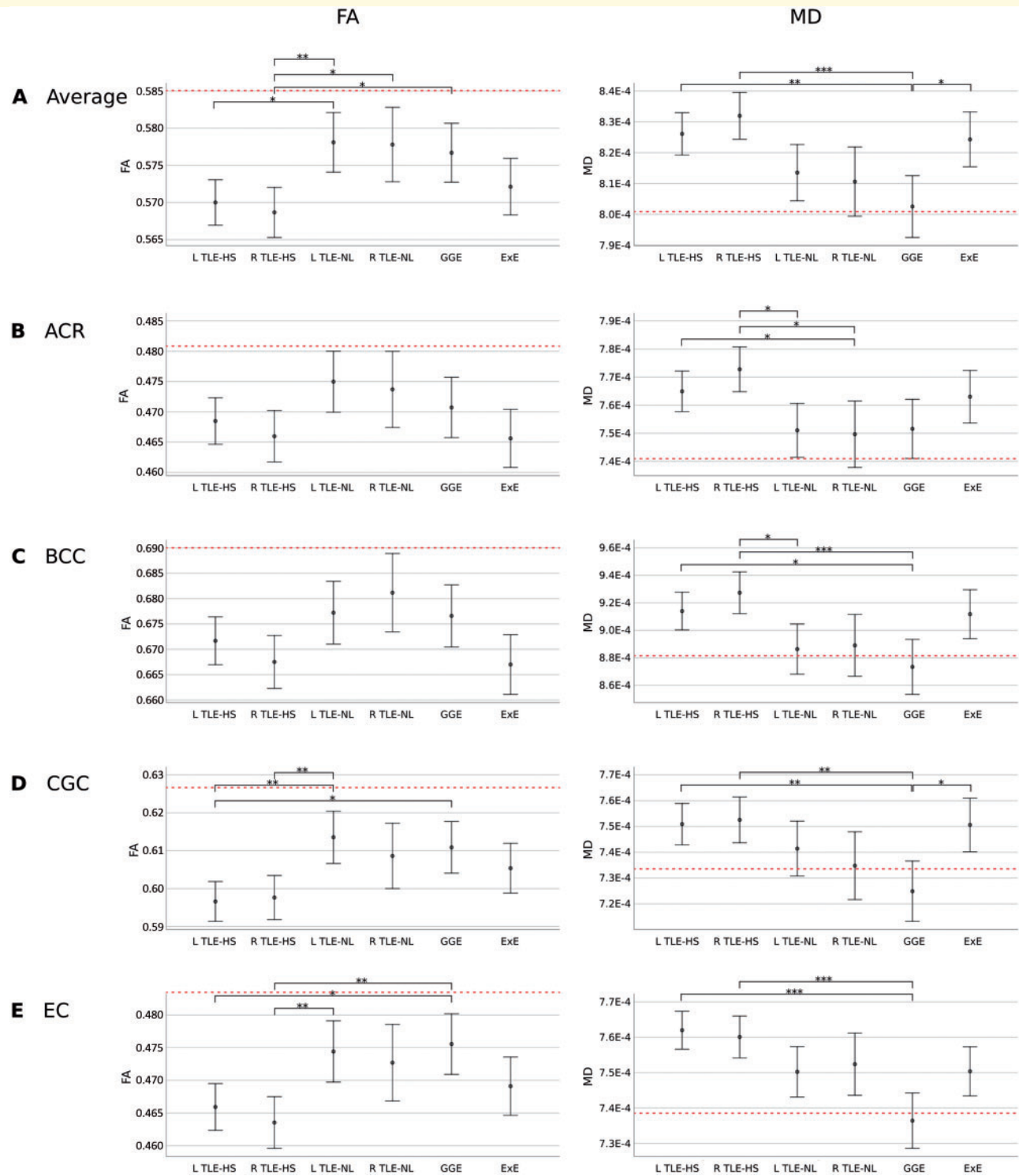


Figure 5 Syndromic difference in average FA and MD in five ROIs. Mean FA (left) and MD (right) for each patient syndrome, controlling for age, age², sex, age of onset, and disease duration. Error bars reflect 95% confidence intervals. Dotted red lines reflect the means of controls. For FA, average = 0.585, ACR = 0.481, BCC = 0.690, CGC = 0.627, external capsule (EC) = 0.484. For MD, average = 0.000801, ACR = 0.000741, BCC = 0.000881, CGC = 0.000733, external capsule = 0.000739. Significant differences are indicated with asterisks (* $P < 0.05$, ** $P < 0.01$, *** $P < 0.001$). L = left; R = right.

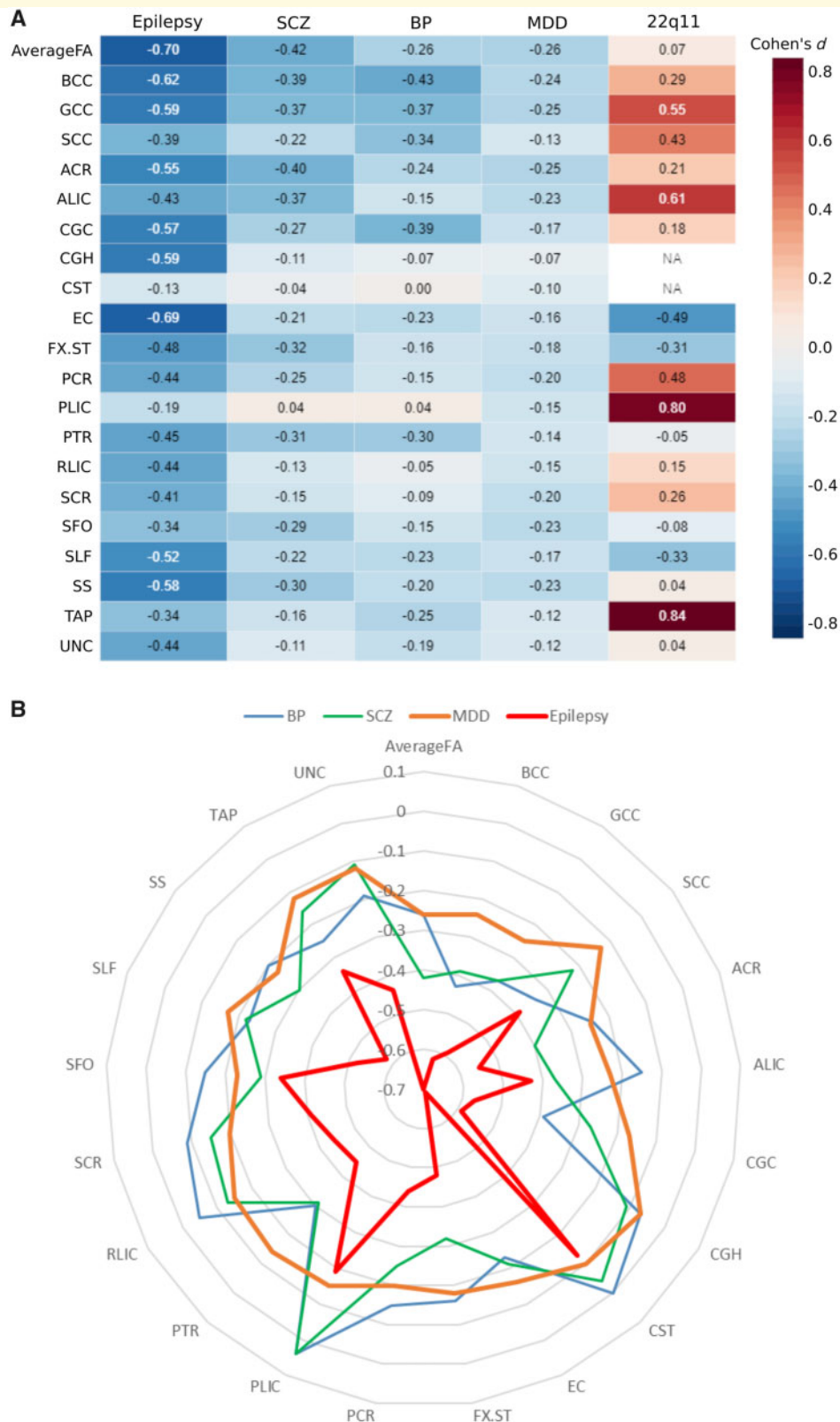


Figure 6 Comparisons of fractional anisotropy measures across neuropsychiatric disorders. (A) Heat map of FA effect sizes for the 'all epilepsies' group compared to those in four other ENIGMA disorders: BP = bipolar disorder; MDD = major depressive disorder; SCZ = schizophrenia. (B) Radar plot of the four disorders that showed significant correlations across white matter tracts. Positive values reflect patient group values were on average higher than controls, whereas negative values reflect cases where patient group values were on average lower than that of controls. ALIC = anterior limb of the internal capsule; CST = corticospinal tract; EC = external capsule; FX.ST = fornix/stria terminalis; PCR = posterior corona radiata; PLIC = posterior limb of the internal capsule; PTR = posterior thalamic radiation; RLIC = rentrolenticular part of the internal capsule; SCR = superior corona radiata; SFO = superior fronto-occipital fasciculus; SS = sagittal stratum; TAP = tapetum; UNC = uncinata.

hypothesize that the white matter changes represent likely secondary effects rather than being causal. However, a prospective longitudinal study of individuals from diagnosis onward is needed to answer this question.

Although previous studies have investigated white matter alterations within a specific epilepsy syndrome, our study is the first to include a diverse aggregation of epilepsy syndromes and address the question of shared brain alterations across syndromes. This analysis revealed widespread reductions in FA across most association, commissural, and projection fibres bilaterally, with smaller effects of increased MD. The most robust alterations were observed in frontocentral regions, including the genu and body of the CC, ACR, CGC, and external capsule. These regional changes mirror results from our structural MRI findings (Whelan *et al.*, 2018), which revealed subcortical atrophy and neocortical thinning in fronto-central, midline structures, including the thalamus, pallidum, pre- and postcentral gyri, and superior frontal regions bilaterally. These regions showed the strongest association with both age of seizure onset and disease duration. Therefore, white matter abnormalities in these regions may be a result of both aberrant developmental [i.e. disruptions of late-myelinating pathways due to seizures (Lee *et al.*, 2013; Ostrowski *et al.*, 2019)] and degenerative [i.e. demyelination and/or axonal loss due to years of epilepsy, recurrent seizures, exposure to AEDs (Günbey *et al.*, 2011)] processes. Although lower FA and higher MD have been interpreted as reflecting a combination of pathological processes, we observed differences across syndromes to be driven primarily by higher RD supporting the concept that disrupted or altered myelin, rather than significant axonal loss, may underlie these changes (Arfanakis *et al.*, 2002; Song *et al.*, 2002; Concha *et al.*, 2009).

Temporal lobe epilepsy

A recent imaging-based meta-analysis (Slinger *et al.*, 2016) found that patients with TLE had pronounced and widespread white matter injury relative to other patient syndromes. We found that this pattern was much more robust and ipsilateral in patients with HS, particularly in hippocampal afferent and efferent tracts, including the CGH, FX/ST, and uncinata. The proximity of these latter white matter regions to the epileptogenic zone, with changes being greater ipsilaterally than contralaterally, implies that these alterations are driven by intrinsic factors specific to the TLE-HS syndrome rather than long-term effects of AEDs. Contrary to prior work (Ahmadi *et al.*, 2009; Whelan *et al.*, 2018), we did not find greater abnormalities in patients with left TLE relative to right TLE in either the TLE-HS or TLE-NL groups, nor did we find greater injury in males with TLE relative to females. Rather, males with TLE-HS and TLE-NL showed higher global FA values relative to females. This contrasts with a previous meta-analysis that found males with focal epilepsy to be more vulnerable to white matter injury relative to females (Slinger *et al.*, 2016). These findings

do not appear to reflect differences in age, age of seizure onset, or disease duration, as these characteristics did not differ between males and females in our TLE cohorts. It has been reported that compared to age-matched females, males have greater white matter volume and neuronal number with fewer neuronal processes (Rabinowicz *et al.*, 1999), which is hypothesized to represent fewer, thicker and more organized fibres in males compared to more crossing fibre tracts in females (Schmithorst *et al.*, 2008). This hypothesis is supported by the finding that higher FA in males compared to females was also observed in our healthy control sample.

Patients with TLE-NL showed a very mild pattern of white matter disruption compared to TLE-HS (Campos *et al.*, 2015) (Figs 3 and 4). Although this may, in part, reflect the greater likelihood for patients with TLE-NL to have a milder form of epilepsy, previous studies have shown that even among drug-resistant TLE, patients with TLE-NL harbour less severe cortical (Bernhardt *et al.*, 2016, 2019) and white matter (Liu *et al.*, 2012) abnormalities compared to TLE-HS. White matter disruptions in TLE-NL were notable in the external capsule and sagittal stratum, both of which contain long-range association pathways. In particular, the sagittal stratum contains fibres of the inferior fronto-occipital fasciculus and the inferior longitudinal fasciculus (Goga *et al.*, 2015). These fibres course through the temporal lobe lateral to the CGH and FX/ST supporting data suggesting that TLE-HS and TLE-NL involve different epileptogenic networks (Zaveri *et al.*, 2001; Mueller *et al.*, 2009). However, many FA/MD alterations did not differ between TLE-HS and TLE-NL patients, once age of seizure onset and disease duration were taken into account (Fig. 5). Thus, the magnitude of these differences appears to be influenced by differences in clinical characteristics. This is supported by the association of an earlier age of seizure onset and longer disease duration with regional white matter disruption in TLE-HS, but not in TLE-NL.

Genetic generalized epilepsy

GGE includes several related syndromes, defined electrophysiologically by generalized, bisynchronous, and symmetric activity with spike-wave or polyspike-wave discharges (Weir, 1965; Seneviratne *et al.*, 2012). These syndromes have traditionally been associated with thalamocortical dysfunction, with some studies reporting atrophy in the thalamus (Whelan *et al.*, 2018) or thalamocortical networks (Bernhardt *et al.*, 2009), and other studies reporting no structural changes relative to controls (McGill *et al.*, 2014). Although patients with GGE showed modest alterations relative to patients with focal epilepsy across most fibres, these differences were broader than those previously observed (Slinger *et al.*, 2016) and include commissural (GCC), projection (ACR) and corticocortical association pathways (external capsule, SLF). In addition, the magnitude of these changes in the ACR was similar to those observed in other epilepsy syndromes after adjusting for clinical and

demographic characteristics (Fig. 5). The ACR is part of the limbic-thalamo-cortical circuitry and includes thalamic projections from the internal capsule to the cortex, including prominent connections to the frontal lobe bilaterally (Catani *et al.*, 2002; Wakana *et al.*, 2004). Thus, degradation of these projection fibres supports the hypothesis that fronto-thalamic pathology is present in patients with GGE, including juvenile myoclonic epilepsy (Woermann *et al.*, 1999; Keller *et al.*, 2011).

Extratemporal epilepsy

The group of patients with non-lesional focal ExE showed the most marked alterations in the BCC, GCC, ACR, CGC, and external capsule, and showed a similar pattern to the GGE group of bilateral fronto-central alterations. As frontal lobe epilepsy is the second most common type of focal epilepsy (Manford *et al.*, 1992), it is likely that this group dominated the ExE group, explaining the predominance of fronto-midline pathology. Unlike the TLE-HS, neither age of seizure onset nor disease duration were associated with regional white matter compromise. This may be related to the heterogeneity of this patient group, their later age of seizure onset and/or the fact that this non-lesional group may represent a ‘mild’ form of ExE.

Summary

In summary, we found shared white matter compromise across epilepsy syndromes, dominated by regional alterations in bilateral midline, fibre bundles. The question arises as to whether these shared alterations are specific to epilepsy or are non-specific effects of a chronic brain disorder. Comparison of our effect size to those of five other ENIGMA populations revealed that the pattern of microstructural compromise in epilepsy was similar to, but more robust than, the patterns observed in bipolar disorder, schizophrenia, and major depressive disorder. In particular, the BCC and GCC were commonly affected across disorders, suggesting that microstructural compromise could reflect a shared patho-physiological mechanism. However, patients with epilepsy tend to have high rates of comorbid mood disorder (Kanner, 2006) and these were not characterized in our epilepsy sample. Therefore, overlap in white matter changes between our epilepsy cohort and major neuropsychiatric disorders could reflect the presence of comorbid psychiatric symptoms in our patients. Increasing evidence suggests that neuropsychiatric disorders themselves are not separated by sharp neurobiological boundaries (Baker *et al.*, 2019), but have overlapping of genetic influences and brain dysfunction (Brainstorm Consortium *et al.*, 2018; Radonjić *et al.*, 2019). Although genetic overlap between these neuropsychiatric disorders and epilepsy is low, overlap in dysfunctional brain networks may be partly due to comorbidities, and warrants further investigation.

Limitations

First, although much effort was taken to apply post-acquisition harmonization, each scanner varied in either its image acquisition protocol or scanner hardware, or both, which increased methodological heterogeneity. Conversely, our results can be considered independent of any specific acquisition scheme, head coil or scanner model. Accordingly, while the absence of a single, standardized magnetic resonance protocol incorporates scanner variance into the data, it also provides breadth that enhances the generalizability of findings. Because some sites had a small sample of patients within a particular syndrome or no control data, we were unable to adequately implement statistical approaches that could specifically address site/sample bias. The statistical batch normalization process ComBat corrected differences between scanner instances, but may not adequately accommodate the heterogeneous neuropathology of epilepsy, resulting in a ‘smoothing out’ of differences between syndromes.

A second limitation is the challenge of directly ascribing lower FA and higher MD to demyelination and/or axonal injury. Specifically, lower FA can reflect the effects of crossing fibres, increases in extracellular diffusion (e.g. inflammation, oedema) or other technical or biological factors. Therefore, advanced diffusion sequences such as high angular resolution diffusion imaging and multi-shell diffusion MRI acquisitions, together with analysis of quantitative contrasts sensitive to tissue microstructural features and neuropathological investigations, would help better unravel the biological underpinnings of our findings.

The GGE and ExE subgroups represented heterogeneous cohorts, which may have contributed to the weaker effects noted in these groups relative to TLE-HS. Although we were underpowered in this study to divide our GGE and ExE patients into more specific syndromes, future studies of more targeted syndromes (i.e. juvenile myoclonic epilepsy) would be beneficial. Similarly, although all patients in our study were diagnosed according to ILAE guidelines, many patients did not receive intracranial EEG (iEEG). In practice, only a very small proportion of people with epilepsy ever have iEEG. Therefore, we cannot rule out the possibility that some patients were misclassified or had multi-focal seizure onsets that were not detected. The lack of iEEG and postoperative outcome data on all participants also made it challenging to further characterize our ExE patients according to seizure laterality or more specific seizure onset, or to confirm that our TLE-NL group did not include patients with seizure arising from other locations. Furthermore, the lack of clinical data prevented us from directly assessing how these diffusional changes were associated with specific AED regimens, comorbid disorders, cognitive performances, or how they relate to clinical outcomes (i.e. drug resistance or post-operative seizure outcome). These data are now being collected across the consortium to better characterize patients and evaluate the clinical utility of identifying

syndrome-specific and shared microstructural injury in epilepsy.

Conclusions and clinical implications

In the largest DTI mega-analysis of epilepsy, we demonstrate a pattern of robust white matter alterations within and across patient syndromes, revealing shared and unique features for each syndrome. These patterns of white matter injury may help to explain cognitive impairments associated with each syndrome [e.g. the extent of memory impairment in TLE has been linked to the extent of CGH and uncinata damage (McDonald *et al.*, 2008)], as well as across syndrome similarities in cognitive profiles [e.g. patients with TLE and GGE both present with executive dysfunction that may reflect their shared fronto-central white matter damage; (Abarrategui *et al.*, 2018; Reyes *et al.*, 2018)]. The extent of microstructural injury may also help to predict postsurgical seizure (Bonilha *et al.*, 2015) and cognitive (McDonald *et al.*, 2014) outcomes, or to inform which patients will respond to AEDs (Park *et al.*, 2020). Finally, cross-syndrome and cross-disease comparisons could help to inform gene expression studies and provide novel insights into shared psychiatric co-morbidities.

Acknowledgements

L.C: We extend our gratitude to the many people who have at some point participated in this study: Juan Ortíz-Retana, Erick Pasaye, Leopoldo González-Santos, Leticia Velázquez-Pérez, David Trejo, Héctor Barragán, Arturo Domínguez, Ildefonso Rodríguez-Leyva, Ana Luisa Velasco, Luis Octavio Jiménez, Daniel Atilano, Elizabeth González Olvera, Rafael Moreno, Vicente Camacho, Ana Elena Rosas, and Alfonso Fajardo.

Funding

S.N.H: NIH R01NS065838; NIH R21NS107739; L.B: R01 NS110347-01A1; E.A: European Union Horizon 2020 research and innovation programme under the Marie Skłodowska-Curie grant agreement no.75088; S.A: This work was part funded by Science Foundation Ireland (16/RC/3948) and was cofunded under the European Regional Development Fund and by FutureNeuro industry partners; A.A holds an MRC eMedLab Medical Bioinformatics Career Development Fellowship. This work was partly supported by the Medical Research Council [grant number MR/L016311/1]; M.K.M.A: FAPESP 15/17066-0; A.R.B: NIH R01NS065838; B.C.B. acknowledges support from CIHR (FDN-154298), SickKids Foundation (NI17-039), Natural Sciences and Engineering Research Council (NSERC; Discovery-1304413), Azrieli Center for Autism Research of

the Montreal Neurological Institute (ACAR), and the Canada Research Chairs program; G.L.C: This work was part funded by Science Foundation Ireland (16/RC/3948) and was cofunded under the European Regional Development Fund and by FutureNeuro industry partners; F.C: The UNICAMP research centre was funded by FAPESP (São Paulo Research Foundation); Contract grant number: 2013/07559-3; L.C: Supported by CONACYT (181508 and 1782); and UNAM-DGAPA (IB201712 and IG200117). Imaging was performed at the National Laboratory for magnetic resonance imaging (CONACYT 232676, 251216, and 280283); O.D: Finding A Cure for Epilepsy and Seizures; J.S.D: National Institute of Health Research; N.K.F: DFG FO750/5-1; S.F.F: CUBRIC, Cardiff University; E.G: R01 NS110347-01A1; K.H: Health and Care Research Wales; A.I: Fapesp-BRAINN (2013/07559-3), Fapesp (2015/17335-0), Fapesp (2016/16355-0); S.S.K: Medical Research Council (MR/S00355X/1 and MR/K023152/1) and Epilepsy Research UK (1085) grants; P.V.K: R01EB015611; B.A.K.K: Epilepsy Action Postgraduate Research Bursary (Research Grants Programme 2014-2015); P.K. is supported by the MRFF Practitioner Fellowship; P.M. was supported by the PATE program (F1315030) of the University of Tübingen; J.C.V.M: FAPESP-BRAINN (2013/07559-3); M.E.M-S: NIH Grant; T.J.O: NHMRC Program Grant (#APP1091593); L.F.R: FAPESP-BRAINN (2013/07559-3); M.P.R: Medical Research Council programme grant (MR/K013998/1); Medical Research Council Centre for Neurodevelopmental Disorders (MR/N026063/1); NIHR Biomedical Research Centre at South London and Maudsely NHS Foundation Trust; C.S.R: FAPESP-BRAINN (07559-3); F.R: CePTER-Grant, LOEWE Programme, Minister of Research and Arts, Hesse, Germany; B.S. is supported by Alfred Health, Monash University and Australian Commonwealth grant ICG000723; P.S: This work was developed within the framework of the DINOGMI Department of Excellence of MIUR 2018-2022 (legge 232 del 2016); R.H.S: Epilepsy Research UK; A.V: Epitarget; S.B.V: National Institute for Health Research University College London Hospitals Biomedical Research Centre (NIHR BRC UCLH/UCL High Impact Initiative BW.mn.BRC10269); G.P.W: Medical Research Council (G0802012), National Institute for Health Research University College London Hospitals Biomedical Research Centre, Epilepsy Society; C.L.I.N.Y: FAPESP-BRAINN (2013/07599-3), CNPQ (403726/2016-6); P.M.T. was funded in part by the United States NIH Big Data to Knowledge (BD2K) program under consortium grant U54 EB020403, the ENIGMA World Aging Center (R56 AG058854), and the ENIGMA Sex Differences Initiative (R01 MH116147); N.J: R01MH117601, R01AG059874, R01MH121246, U54EB020403, P41EB015922; S.M.S: The work was partly undertaken at UCLH/UCL, which received a proportion of funding from the Department of Health's NIHR Biomedical Research Centres funding scheme. We are grateful to the Wolfson Trust and the Epilepsy Society for supporting the Epilepsy Society MRI scanner; C.R.M: NIH R01NS065838; NIH R21NS107739.

Competing interests

N.K.F. has received honoraria by Bial, EGI, Eisai, and UCB. R.H.T. has received honoraria from Eisai, GW Pharma, Sanofi, UCB Pharma, Zogenix and meeting support from Bial, LivaNova, and Novartis. P.S. has received honoraria from Eisai, Kolfarma, GW Pharma, Biomarin, Lusofarma, Zogenix and meeting support from Kolfarma, GW pharma, Biomarin. P.M.T. received partial grant support from Biogen, Inc. (USA) for research unrelated to this manuscript. N.J. is MPI of a research grant from Biogen, Inc., for work unrelated to the contents of this manuscript. F.C. received honoraria by UCB. All other authors report no competing interests.

Supplementary material

Supplementary material is available at *Brain* online.

References

- Abarrategui B, Parejo-Carbonell B, García García ME, Di Capua D, García-Morales I. The cognitive phenotype of idiopathic generalized epilepsy. *Epilepsy Behav* 2018; 89: 99–104.
- Ahmadi ME, Hagler DJ, McDonald CR, Tecoma ES, Iragui VJ, Dale AM, et al. Side matters: diffusion tensor imaging tractography in left and right temporal lobe epilepsy. *AJNR Am J Neuroradiol* 2009; 30: 1740–7.
- Altmann A, Ryten M, Nunzio MD, Ravizza T, Tolomeo D, Reynolds RH, et al. A systems-level analysis highlights microglial activation as a modifying factor in common forms of human epilepsy bioRxiv 2017: 470518. doi: 10.1101/470518.
- Arfanakis K, Hermann BP, Rogers BP, Carew JD, Seidenberg M, Meyerand ME. Diffusion tensor MRI in temporal lobe epilepsy. *Magn Reson Imaging* 2002; 20: 511–9.
- Baker JT, Dillon DG, Patrick LM, Roffman JL, Brady RO, Pizzagalli DA, et al. Functional connectivities of affective and psychotic pathology. *Proc Natl Acad Sci USA* 2019; 116: 9050–9.
- Bell GS, Neligan A, Sander JW. An unknown quantity—the worldwide prevalence of epilepsy. *Epilepsia* 2014; 55: 958–62.
- Berg AT, Berkovic SF, Brodie MJ, Buchhalter J, Cross JH, van Emde Boas W, et al. Revised terminology and concepts for organization of seizures and epilepsies: report of the ILAE Commission on Classification and Terminology, 2005-2009. *Epilepsia* 2010; 51: 676–85.
- Bernhardt BC, Bernasconi A, Liu M, Hong S-J, Caldirou B, Goubran M, et al. The spectrum of structural and functional imaging abnormalities in temporal lobe epilepsy. *Ann Neurol* 2016; 80: 142–53.
- Bernhardt BC, Fadaie F, Liu M, Caldirou B, Gu S, Jefferies E, et al. Temporal lobe epilepsy: hippocampal pathology modulates connectome topology and controllability. *Neurology* 2019; 92: e2209–e2220.
- Bernhardt BC, Rozen DA, Worsley KJ, Evans AC, Bernasconi N, Bernasconi A. Thalamo-cortical network pathology in idiopathic generalized epilepsy: insights from MRI-based morphometric correlation analysis. *Neuroimage* 2009; 46: 373–81.
- Boedhoe PSW, Heymans MW, Schmaal L, Abe Y, Alonso P, Ameis SH, et al. An empirical comparison of meta- and mega-analysis with data from the ENIGMA obsessive-compulsive disorder working group. *Front Neuroinform* 2018; 12: 102.
- Bonilha L, Jensen JH, Baker N, Breedlove J, Nesland T, Lin JJ, et al. The brain connectome as a personalized biomarker of seizure outcomes after temporal lobectomy. *Neurology* 2015; 84: 1846–53.
- Brainstorm Consortium, Anttila V, Bulik-Sullivan B, Finucane HK, Walters RK, Bras J, et al. Analysis of shared heritability in common disorders of the brain. *Science* 2018; 360: eaap8757.
- Caligiuri ME, Labate A, Cherubini A, Mumoli L, Ferlazzo E, Aguglia U, et al. Integrity of the corpus callosum in patients with benign temporal lobe epilepsy. *Epilepsia* 2016; 57: 590–6.
- Campos BM, Coan AC, Beltramini GC, Liu M, Yassuda CL, Ghizoni E, et al. White matter abnormalities associate with type and localization of focal epileptogenic lesions. *Epilepsia* 2015; 56: 125–32.
- Catani M, Howard RJ, Pajevic S, Jones DK. Virtual in vivo interactive dissection of white matter fasciculi in the human brain. *Neuroimage* 2002; 17: 77–94.
- Coan AC, Cendes F. Understanding the spectrum of temporal lobe epilepsy: contributions for the development of individualized therapies. *Expert Rev Neurother* 2013; 13: 1383–94.
- Concha L, Beaulieu C, Collins DL, Gross DW. White-matter diffusion abnormalities in temporal-lobe epilepsy with and without mesial temporal sclerosis. *J Neurol Neurosurg Psychiatry* 2009; 80: 312–9.
- Engel J, Thompson PM, Stern JM, Staba RJ, Bragin A, Mody I. Connectomics and epilepsy. *Curr Opin Neurol* 2013; 26: 186–94.
- Focke NK, Yogarajah M, Bonelli SB, Bartlett PA, Symms MR, Duncan JS. Voxel-based diffusion tensor imaging in patients with mesial temporal lobe epilepsy and hippocampal sclerosis. *Neuroimage* 2008; 40: 728–37.
- Fortin J-P, Parker D, Tunç B, Watanabe T, Elliott MA, Ruparel K, et al. Harmonization of multi-site diffusion tensor imaging data. *Neuroimage* 2017; 161: 149–70.
- Gleichgerricht E, Munsell B, Bhatia S, Vandergrift WA, Rorden C, McDonald C, et al. Deep learning applied to whole-brain connectome to determine seizure control after epilepsy surgery. *Epilepsia* 2018; 59: 1643–54.
- Goga C, Brinzaniuc K, Florian I, Rodriguez MR. The three-dimensional architecture of the internal capsule of the human brain demonstrated by fiber dissection technique. *ARS Medica Tomitana* 2015; 20: 115–22.
- Günbey HP, Ercan K, Findıkoğlu AS, Bilir E, Karaoglanoglu M, Komurcu F, et al. Secondary corpus callosum abnormalities associated with antiepileptic drugs in temporal lobe epilepsy. A diffusion tensor imaging study. *Neuroradiol J* 2011; 24: 316–23.
- ILAE. Genome-wide mega-analysis identifies 16 loci and highlights diverse biological mechanisms in the common epilepsies. *Nat Commun* 2018; 9: 5269.
- Jahanshad N, Kochunov PV, Sprooten E, Mandl RC, Nichols TE, Almasy L, et al. Multi-site genetic analysis of diffusion images and voxelwise heritability analysis: a pilot project of the ENIGMA-DTI working group. *Neuroimage* 2013; 81: 455–69.
- Johnson WE, Li C, Rabinovic A. Adjusting batch effects in microarray expression data using empirical Bayes methods. *Biostatistics* 2007; 8: 118–27.
- Kanner AM. Mood disorder and epilepsy: a neurobiologic perspective of their relationship. *Dialog- Clin. Neurosci* 2006; 10: 39–45.
- Keller SS, Ahrens T, Mohammadi S, Möddel G, Kugel H, Ringelstein EB, et al. Microstructural and volumetric abnormalities of the putamen in juvenile myoclonic epilepsy. *Epilepsia* 2011; 52: 1715–24.
- Keller SS, Glenn GR, Weber B, Kreilkamp BAK, Jensen JH, Helpert JA, et al. Preoperative automated fibre quantification predicts postoperative seizure outcome in temporal lobe epilepsy. *Brain* 2017; 140: 68–82.
- Keller SS, Richardson MP, Schoene-Bake J-C, O’Muircheartaigh J, Elkommos S, Kreilkamp B, et al. Thalamotemporal alteration and postoperative seizures in temporal lobe epilepsy. *Ann Neurol* 2015; 77: 760–74.
- Kochunov P, Jahanshad N, Marcus D, Winkler A, Sprooten E, Nichols TE, et al. Heritability of fractional anisotropy in human white matter: a comparison of Human Connectome Project and ENIGMA-DTI data. *Neuroimage* 2015; 111: 300–11.

- Kochunov P, Jahanshad N, Sprooten E, Nichols TE, Mandl RC, Almasy L, et al. Multi-site study of additive genetic effects on fractional anisotropy of cerebral white matter: comparing meta and mega-analytical approaches for data pooling. *Neuroimage* 2014; 95: 136–50.
- Labate A, Cherubini A, Tripepi G, Mumoli L, Ferlazzo E, Aguglia U, et al. White matter abnormalities differentiate severe from benign temporal lobe epilepsy. *Epilepsia* 2015; 56: 1109–16.
- Lebel C, Gee M, Camicioli R, Wieler M, Martin W, Beaulieu C. Diffusion tensor imaging of white matter tract evolution over the lifespan. *Neuroimage* 2012; 60: 340–52.
- Lee C-Y, Tabesh A, Benitez A, Helpert JA, Jensen JH, Bonilha L. Microstructural integrity of early- versus late-myelinating white matter tracts in medial temporal lobe epilepsy. *Epilepsia* 2013; 54: 1801–9.
- Lee C-Y, Tabesh A, Spampinato MV, Helpert JA, Jensen JH, Bonilha L. Diffusional kurtosis imaging reveals a distinctive pattern of microstructural alternations in idiopathic generalized epilepsy. *Acta Neurol Scand* 2014; 130: 148–55.
- Liu M, Concha L, Lebel C, Beaulieu C, Gross DW. Mesial temporal sclerosis is linked with more widespread white matter changes in temporal lobe epilepsy. *Neuroimage Clin* 2012; 1: 99–105.
- Manford M, Hart YM, Sander JW, Shorvon SD. National General Practice Study of Epilepsy (NGPSE): partial seizure patterns in a general population. *Neurology* 1992; 42: 1911–7.
- McDonald CR, Ahmadi ME, Hagler DJ, Tecoma ES, Iragui VJ, Gharapetian L, et al. Diffusion tensor imaging correlates of memory and language impairments in temporal lobe epilepsy. *Neurology* 2008; 71: 1869–76.
- McDonald CR, Leyden KM, Hagler DJ, Kucukboyaci NE, Kemmotsu N, Tecoma ES, et al. White matter microstructure complements morphometry for predicting verbal memory in epilepsy. *Cortex* 2014; 58: 139–50.
- McGill ML, Devinsky O, Wang X, Quinn BT, Pardoe H, Carlson C, et al. Functional neuroimaging abnormalities in idiopathic generalized epilepsy. *Neuroimage Clin* 2014; 6: 455–62.
- Mueller SG, Laxer KD, Barakos J, Cheong I, Garcia P, Weiner MW. Widespread neocortical abnormalities in temporal lobe epilepsy with and without mesial sclerosis. *Neuroimage* 2009; 46: 353–9.
- Ostrowski LM, Song DY, Thorn EL, Ross EE, Stoyell SM, Chinappen DM, et al. Dysmature superficial white matter microstructure in developmental focal epilepsy. *Brain Commun* 2019; 1: fcz002.
- Otte WM, van Eijsden P, Sander JW, Duncan JS, Dijkhuizen RM, Braun K. A meta-analysis of white matter changes in temporal lobe epilepsy as studied with diffusion tensor imaging. *Epilepsia* 2012; 53: 659–67.
- Park KM, Cho KH, Lee H-J, Heo K, Lee BI, Kim SE. Predicting the antiepileptic drug response by brain connectivity in newly diagnosed focal epilepsy. *J Neurol* 2020; 267: 1179–87.
- Rabinowitz T, Dean DE, Petetot JM, de Courten-Myers GM. Gender differences in the human cerebral cortex: more neurons in males; more processes in females. *J Child Neurol* 1999; 14: 98–107.
- Radonjić NV, Hess JL, Rovira P, Andreassen O, Buitelaar JK, Ching CRK, et al. Structural brain imaging studies offer clues about the effects of the shared genetic etiology among neuropsychiatric disorders. *bioRxiv* 2019; 809582. doi: 10.1101/809582.
- Reyes A, Uttarwar VS, Chang Y-H, Balachandra AR, Pung CJ, Hagler DJ, et al. Decreased neurite density within frontostriatal networks is associated with executive dysfunction in temporal lobe epilepsy. *Epilepsy Behav* 2018; 78: 187–93.
- Sawilowsky SS. New effect size rules of thumb. *J Mod Appl Stat Methods* 2008; 8.
- Scheffer IE, Berkovic S, Capovilla G, Connolly MB, French J, Guilhotto L, et al. ILAE classification of the epilepsies: position paper of the ILAE Commission for Classification and Terminology. *Epilepsia* 2017; 58: 512–21.
- Schmithorst VJ, Holland SK, Dardzinski BJ. Developmental differences in white matter architecture between boys and girls. *Hum Brain Mapp* 2008; 29: 696–710.
- Seneviratne U, Cook M, D'Souza W. The electroencephalogram of idiopathic generalized epilepsy. *Epilepsia* 2012; 53: 234–48.
- Slinger G, Sinke MRT, Braun KPJ, Otte WM. White matter abnormalities at a regional and voxel level in focal and generalized epilepsy: a systematic review and meta-analysis. *Neuroimage Clin* 2016; 12: 902–9.
- Song S-K, Sun S-W, Ramsbottom MJ, Chang C, Russell J, Cross AH. Dysmyelination revealed through MRI as increased radial (but unchanged axial) diffusion of water. *Neuroimage* 2002; 17: 1429–36.
- Szaflarski JP, Lee S, Allendorfer JB, Gaston TE, Knowlton RC, Pati S, et al. White matter abnormalities in patients with treatment-resistant genetic generalized epilepsies. *Med Sci Monit* 2016; 22: 1966–75.
- Téllez-Zenteno JF, Hernández-Ronquillo L. A review of the epidemiology of temporal lobe epilepsy. *Epilepsy Res Treat* 2012; 2012: 630853.
- Thompson PM, Jahanshad N, K Ching CR, Salminen LE, Thomopoulos SI, Bright J, et al. ENIGMA and global neuroscience: a decade of large-scale studies of the brain in health and disease across more than 40 Countries: A Decade of Large-Scale Studies of the Brain in Health and Disease across more than 40 Countries. *Transl Psychiatry* 2020; 10.
- Villalón-Reina JE, Martínez K, Qu X, Ching CRK, Nir TM, Kothapalli D, et al. Altered white matter microstructure in 22q11.2 deletion syndrome: a multisite diffusion tensor imaging study. *Mol Psychiatry* 2019; doi: 10.1038/s41380-019-0450-0.
- Wakana S, Jiang H, Nagae-Poetscher LM, van Zijl PC, Mori S. Fiber tract-based atlas of human white matter anatomy. *Radiology* 2004; 230: 77–87.
- Weir B. The morphology of the spike-wave complex. *Electroencephalogr Clin Neurophysiol* 1965; 19: 284–90.
- Whelan CD, Altmann A, Botía JA, Jahanshad N, Hibar DP, Absil J, et al. Structural brain abnormalities in the common epilepsies assessed in a worldwide ENIGMA study. *Brain* 2018; 141: 391–408.
- Winkler AM, Ridgway GR, Webster MA, Smith SM, Nichols TE. Permutation inference for the general linear model. *Neuroimage* 2014; 92: 381–97.
- Winkler AM, Webster MA, Vidaurre D, Nichols TE, Smith SM. Multi-level block permutation. *Neuroimage* 2015; 123: 253–68.
- Woermann FG, Free SL, Koepp MJ, Sisodiya SM, Duncan JS. Abnormal cerebral structure in juvenile myoclonic epilepsy demonstrated with voxel-based analysis of MRI. *Brain* 1999; 122: 2101–8.
- Yogarajah M, Focke NK, Bonelli SB, Thompson P, Vollmar C, McEvoy AW, et al. The structural plasticity of white matter networks following anterior temporal lobe resection. *Brain* 2010; 133: 2348–64.
- Yogarajah M, Powell HWR, Parker GJM, Alexander DC, Thompson PJ, Symms MR, et al. Tractography of the parahippocampal gyrus and material specific memory impairment in unilateral temporal lobe epilepsy. *Neuroimage* 2008; 40: 1755–64.
- Zavaliangos-Petropulu A, Nir TM, Thomopoulos SI, Reid RI, Bernstein MA, Borowski B, et al. Diffusion MRI indices and their relation to cognitive impairment in brain aging: the updated multi-protocol approach in ADNI3. *Front Neuroinformatics* 2019; 13.
- Zaveri HP, Duckrow RB, de Lanerolle NC, Spencer SS. Distinguishing subtypes of temporal lobe epilepsy with background hippocampal activity. *Epilepsia* 2001; 42: 725–30.